
Continuous Seismic Reflexion Profiles in the Red Sea

J. D. Phillips and D. A. Ross

Phil. Trans. R. Soc. Lond. A 1970 **267**, 143-152

doi: 10.1098/rsta.1970.0029

Email alerting service

Receive free email alerts when new articles cite this article - sign up in the box at the top right-hand corner of the article or click [here](#)

Phil. Trans. Roy. Soc. Lond. A. **267**, 143–152 (1970) [143]

Printed in Great Britain

Continuous seismic reflexion profiles in the Red Sea†

BY J. D. PHILLIPS AND D. A. ROSS

*Woods Hole Oceanographic Institution, Woods Hole,
Massachusetts 02543, U.S.A.*

[Plates 9 to 14]

Twenty continuous seismic reflexion profiles have been made across the main trough of the Red Sea north of 17° N latitude. The main trough is characterized by mildly deformed sediment layers along the margins with highly disturbed materials in the deeper axial trough. A strong seismic reflector is observed at depths up to 500 m beneath the main trough, but is not found in the axial trough. This reflector may represent an unconformity of late Miocene–Early Pliocene age (5 to 6 Ma ago). On the assumption that this unconformity was once continuous across the main trough but has subsequently rifted apart as a result of seafloor spreading in the axial trough, separation distances of 48 to 74 km across the trough imply a minimum seafloor spreading rate of 0.4 to 0.7 cm a⁻¹. This rate is lower than spreading rates inferred from magnetic anomaly profiles in the Red Sea; however, if separation began as late as 2 to 3 Ma ago which can be inferred from the seismic profiles, a rate of 1.4 to 0.9 cm a⁻¹ is indicated. This rate is in good agreement with those determined from magnetic profiles.

INTRODUCTION

The rift structure beneath the Red Sea has been recognized by many workers in recent years (Swartz & Arden 1960; Drake & Girdler 1964; Girdler 1958, 1963, 1966, 1969). Drake & Girdler (1964) proposed that crustal separation accompanied by the intrusion of dense basic rocks beneath the axial trough is responsible for the formation of the rift. Girdler (1966), Laughton (1966), Freund, Zak & Garfunkel (1968), Le Pichon & Heirtzler (1968) and McKenzie (this volume, p. 393) demonstrated, on the basis of strike-slip fault displacements along the Aqaba–Dead Sea rift and across the Gulf of Aden and Northwest Indian Ocean, that simple horizontal motions of the Arabian and African blocks on the order of 60 to 250 km could account for the opening of the Red Sea. Reconstructions by Abdel-Gawad (1969, and this volume, p. 23), Beydoun (this volume, p. 267) and Quennell (1958) of displaced geological structures across the region also support such inferred motions.

Reconnaissance seismic reflexion studies in the Red Sea led Knott, Bunce & Chase (1966) to postulate that deformation of the axial trough may have begun as early as the beginning of Pliocene time. This deformation appears to have been preceded by a long period of sediment deposition across the region.

Vine (1966) found the magnetic anomalies profiles over the southern Red Sea to be compatible with simulated profiles generated by seafloor spreading models. He hypothesized that spreading at a rate of about 1 cm a⁻¹ in a NE–SW direction has been active in the axial trough over the last 2 to 3 Ma. From an examination of reconnaissance magnetic profiles across the axial trough between 25 and 17° N latitude, Phillips (this volume, p. 205) and Phillips, Woodside & Bowin (1969) deduced that seafloor spreading at a rate of 1.6 cm a⁻¹ in a north-northeast direction could also explain the observed anomaly pattern and inferred crustal separation distances. They suggested that multiple seafloor spreading axes, offset by *en échelon* transform

† Contribution no. 2333 of the Woods Hole Oceanographic Institution.

faults, can account for the separation of Arabia and Africa. Sykes (1968) and Fairhead & Girdler (this volume, p. 49) have recently observed earthquake motions with northeast-southwesterly strike-slip motions at appropriate locations that are compatible with transform faulting. More recently, the volcanic nature of the axial trough and its similarity to the mid-oceanic ridges has been documented by several workers investigating the hot brine region in the axial trough near 21° N latitude (see Degens & Ross 1969).

In view of the accumulated evidence there seems little doubt that the formation of the Red Sea has resulted from the crustal separation of Africa and Arabia. However, the amount of separation and whether this separation was produced by simple horizontal motion associated with a single phase of rifting during the last few million years is not altogether clear.

The purpose of this paper is to present continuous seismic reflexion profiles (c.s.p.) obtained during R.V. *Chain* Cruise 61 in 1966, and examine these and previous profiles in an effort to determine from sediment deformation the chronology of seafloor spreading in the Red Sea. This information is the first direct evidence from the Red Sea itself that supports a spreading origin for the axial trough. Although the origin of the main trough is probably related to that of the axial trough, the information contained in our seismic profiles is not considered relevant to this problem.

METHODS AND INSTRUMENTATION

In 1966 during *Chain* Cruise 61 east-west oriented profiles were made to supplement the earlier coverage obtained during *Chain* Cruise 43 in 1964 (figure 1). The seismic profiling instrumentation was essentially the same for both cruises (Knott *et al.* 1966). Line drawing interpretations of each original p.g.r. record were developed in the following manner: solid lines indicate continuously received echoes of similar signal shape; broken lines indicate interrupted reflectors or reflectors of doubtful correlation; broad lines indicate strong reflectors. Corrections have been made for varying ship and recorder paper speeds to provide profiles of uniform horizontal scale. These drawings and those presented by Knott *et al.* (1966) form the basis of the analyses presented here.

RESULTS

The location of continuous seismic reflexion profiles in the Red Sea is shown in figure 1 together with a generalized bathymetric contour chart modified from British Admiralty Chart no. C 6359. The three physiographic provinces: coastal shelves, main trough, and deep axial trough as recognized by Drake & Girdler (1964) and others, are roughly enclosed by the shoreline and the 300- and 700-fathom contours (547 and 1280 m) respectively. The seismic profiles are generally restricted to the region of the main and axial troughs. The main trough is continuous from the Gulf of Aqaba near 28° N latitude south to about 15° N latitude. A continuous axial trough is restricted to the region south of 24° N latitude. Between 28 and 24° N only isolated deeps characteristic of the axial trough are found.

Photographs of the recorded seismic profiles made during *Chain* Cruise 61 together with their line drawing interpretations are shown in figures 2 to 16, plates 9 to 13. The profiles across the entire main trough north of 24° N (figures 2 to 8) and over its extreme east and west margins between 18 and 25° N latitude (figures 9 to 16) show thick sequences of gently folded strata (up to 1 s penetration). These strata include a prominent strong reflector, termed S, at about 0.4 s (330 m) below the seafloor. The detailed nature of this strong subbottom reflector is shown in sections of certain *Chain* 43 profiles (figures 17 to 19, plates 13 and 14).

Between 23 and 27° N latitude the dominant deformation of the layers in the central portion of the main trough appears as minor offset of the reflector sequences and broad regional folds. Local tightly folded sequences are contained within basin structures and the broader folds of reflector S (figures 2 to 9). In only a few places is the characteristic reflector S entirely absent (figure 9, and figures 10 and 12 in Knott *et al.* 1966). In the profiles north of 23° N latitude

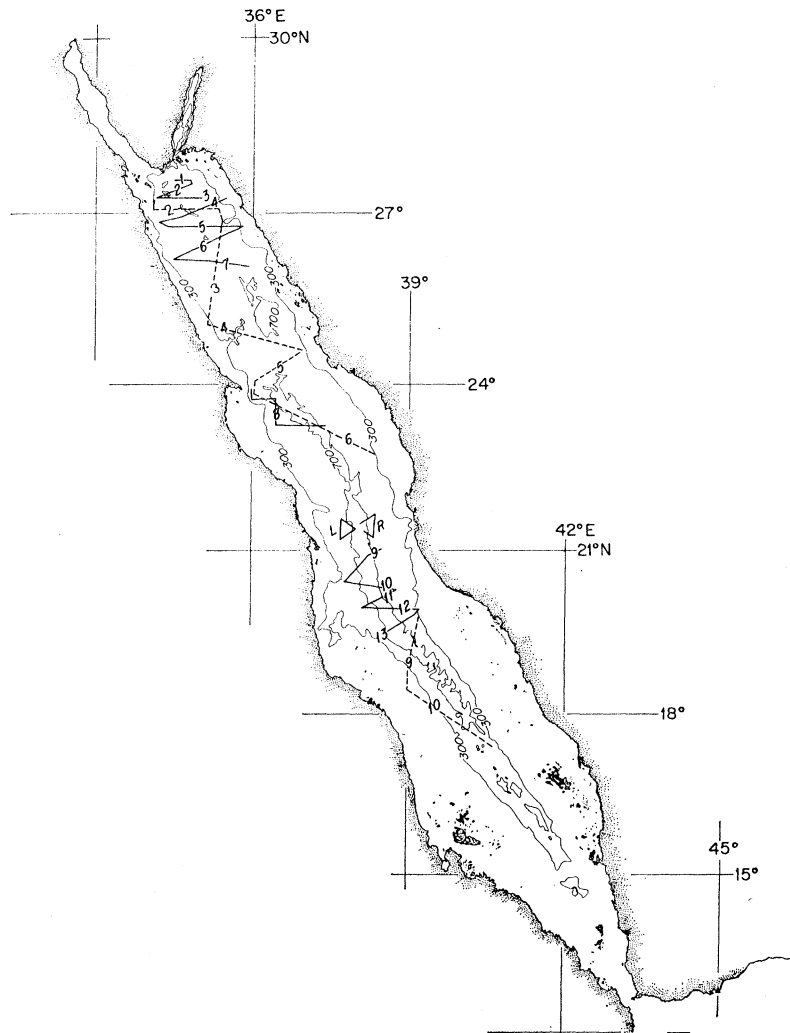


FIGURE 1. Index map of Red Sea showing location of continuous seismic reflexion profiles. Solid lines indicate the Chain 61 profiles of figures 2 to 16. Chain 43 profiles previously reported by Knott *et al.* (1966) are shown as dotted lines.

narrow crevasses about 100 m deep, above disturbed reflectors, are common across the centre of the main trough. These features have been indicated by a cross above the profiles (figures 2 to 9). Similar crevasses are shown in the profiles of Knott *et al.* (1966).

The uniform character of reflector S should be emphasized. It is generally a distinct multiple echo sequence extending over a 0.1 to 0.2 s time interval, much like the sequence returning from the seafloor (figures 17 and 18). The attitude of this reflector with respect to the layers above and below should also be noted. In the flank regions of the main trough the reflecting horizons beneath appear to parallel it in a continuous manner, while the reflecting sequences

above, directly beneath the seafloor, are more flat lying. In some profiles a thin sequence above reflector S seems to be folded conformably with reflector S (for example, figures 3, 4, 7, 8 and 14). Also, there is little correspondence between the configuration of reflector S and the seafloor topography (figures 3 to 8 and 12 to 18). The average thickness of materials above reflector S is relatively uniform across the flanks of the main trough.

In contrast to these marginal regions, the central portions of the profiles north of about 25° N and those across the main/axial trough boundary show reflector S to shape the seafloor topography (figures 5 to 9, 11 to 16 and 19), and the total thickness of the layers above reflector S appears to decrease gradually toward the axial trough (figures 11 to 15). In addition, the thick-layered sequence beneath reflector S abruptly disappears (figures 9 to 14 and 17). In several places reflector S appears to onlap acoustically opaque material, eventually becoming indistinguishable from this underlying opaque material (figures 7 to 9 and 17). In certain other profiles it appears to crop out on the steep walls of the axial trough (figures 11 and 14). Reflector S can usually be traced to within 5 to 10 km of the axial trough.

The thick-layered materials common to the main trough are virtually absent in the axial trough (figures 10 to 16). However, isolated patches containing a thin sequence of reflectors are found along the acoustically opaque walls of the axial trough (figures 10 and 12). Also, small areas of material, acoustically transparent as compared to the reflecting sequences along the margins of the main trough, are found in ponds of the axial trough and along its upper slopes (figures 11 to 16). This transparent material appears to be a relatively continuous layer along the slopes. Its upper surface, the seafloor, closely follows the configuration of the opaque material beneath (figure 19). The transparent layer extends landward from the axial trough and gradually merges with the typical layered sequences found above the reflector S on the margins of the main trough (figures 11 to 16). Reflector S has not been observed in the axial trough.

DISCUSSION

The marked differences in the subbottom reflectors beneath the various parts of the Red Sea bear strongly on ideas concerning the origin of the axial trough. The thick-layered sequence along the margins provides evidence for a long history for the main trough. Information from land outcrops, boreholes along the Egyptian and Arabian Coast, and from seismic refraction (Brown, this volume, p. 75; Davies & Tramontini, p. 181; Frazier, p. 131; Said 1962, pp. 107–119; and Drake & Girdler 1964) shows that a thick sequence of Upper Tertiary sediments extends seaward beneath the coastal shelves and main trough of the entire Red Sea. It is generally believed that strong tectonic activity at the end of Miocene time terminated the deposition of

DESCRIPTION OF PLATES 9 TO 13

FIGURES 2 to 16 (Plates 9 to 13). Continuous seismic reflexion profiles 1–13, L and R. The top portion of each figure is a photograph of the original record; the bottom is a line drawing interpretation of the record. Vertical scales are: (left hand) one-way travel time (seconds) of received signals and (right hand) depth (kilometres) based on an assumed velocity of 1.5 km s⁻¹ for both water and subbottom materials. The vertical exaggeration of the bathymetry is about 20:1; that of the subbottom layer configuration somewhat less. The location of each profile can be seen in figure 1, p. 145. The letter symbols in each of the line drawings refer to disturbed Pliocene layers (P) just above reflector S along the margins of the main trough: the thin reflecting sequences R in the axial trough, the strong subbottom reflector S, the transparent materials T, and the narrow crevasses X associated with disturbed subbottom features. The latter are believed to be sections across strike-slip fault planes.

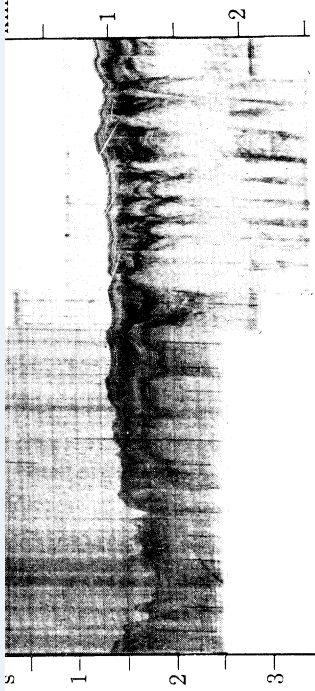


FIGURE 2

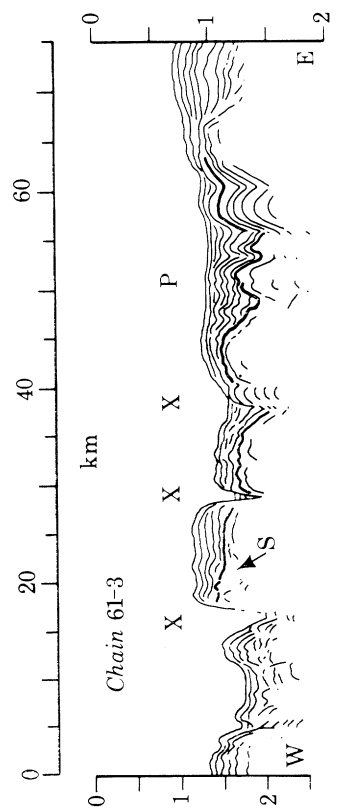
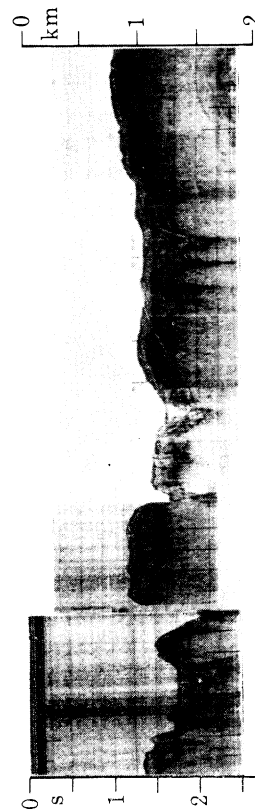


FIGURE 4

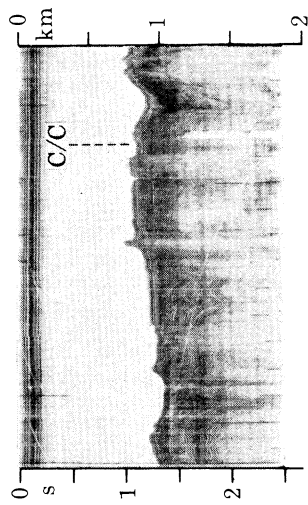


FIGURE 3

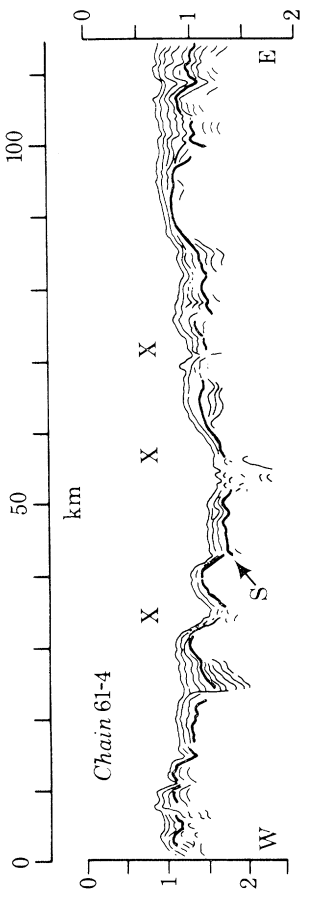
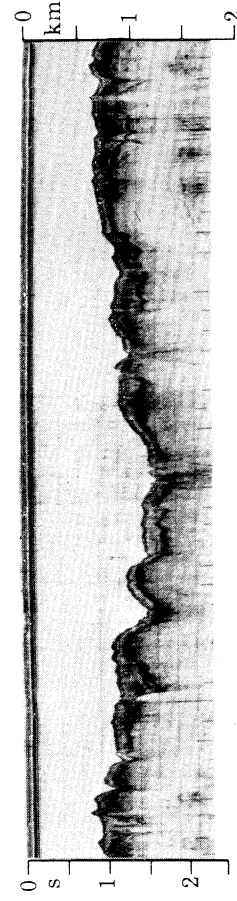
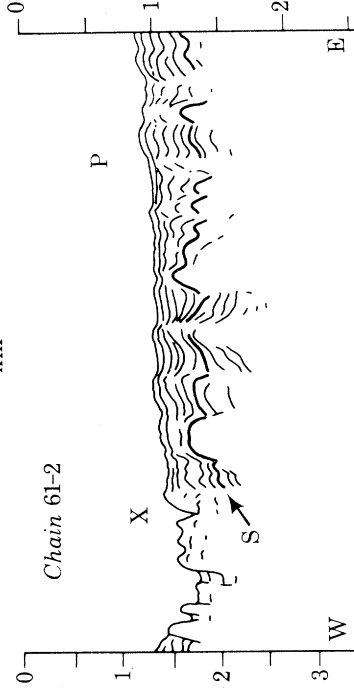


FIGURE 5

For legends see facing page.

FIGURE 6

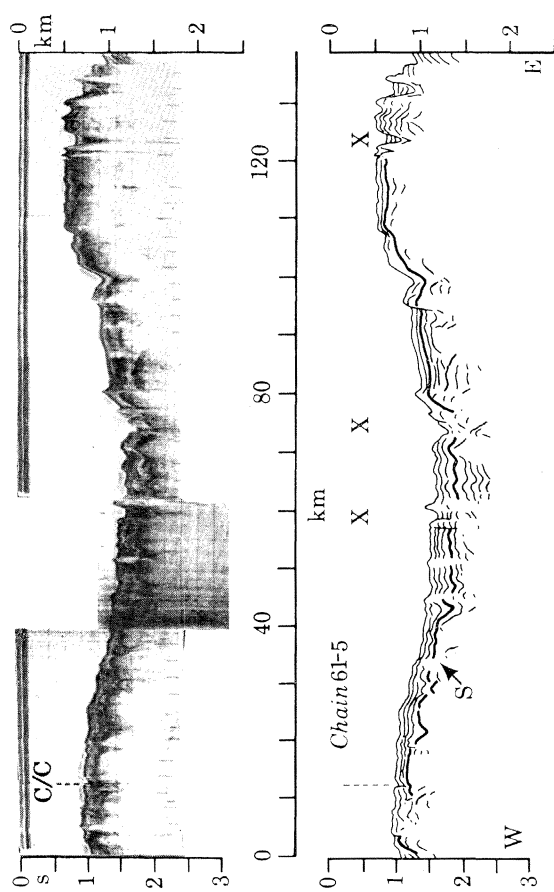


FIGURE 7

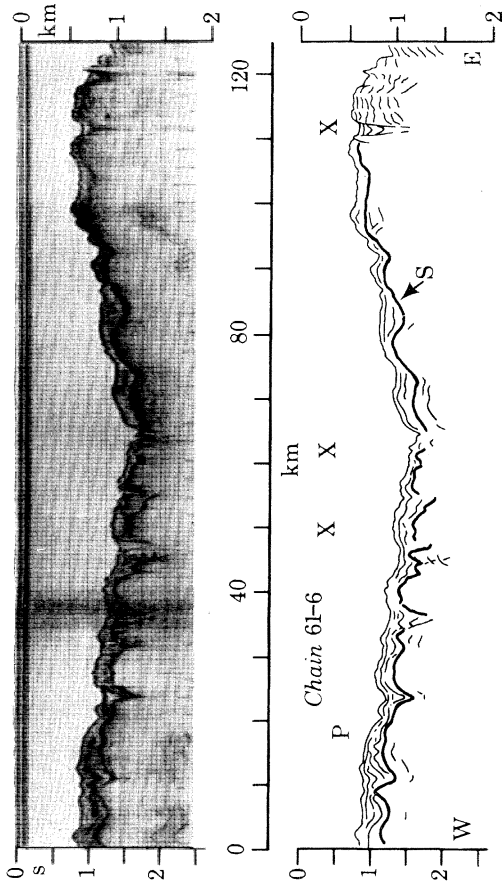


FIGURE 8

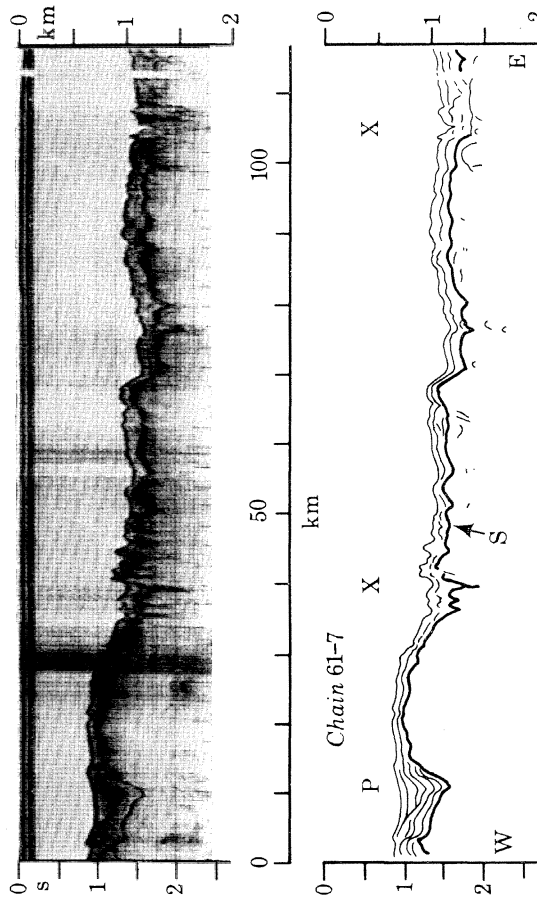
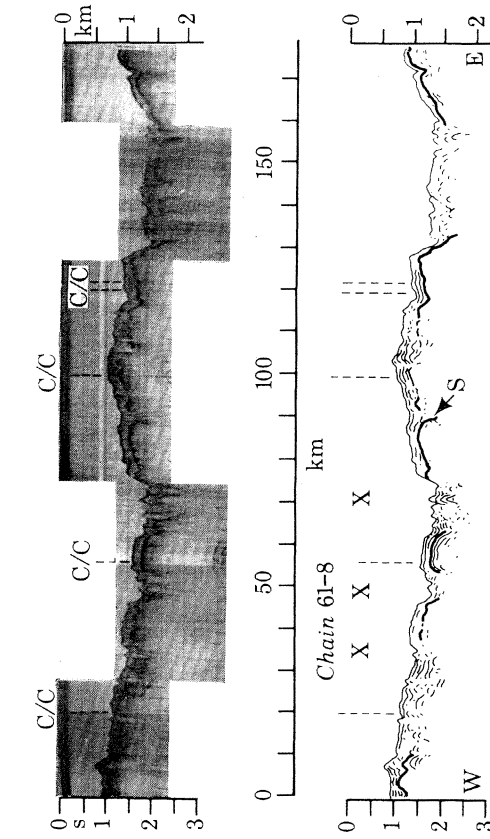


FIGURE 9



For legends see p. 146.

FIGURE 8

FIGURE 9

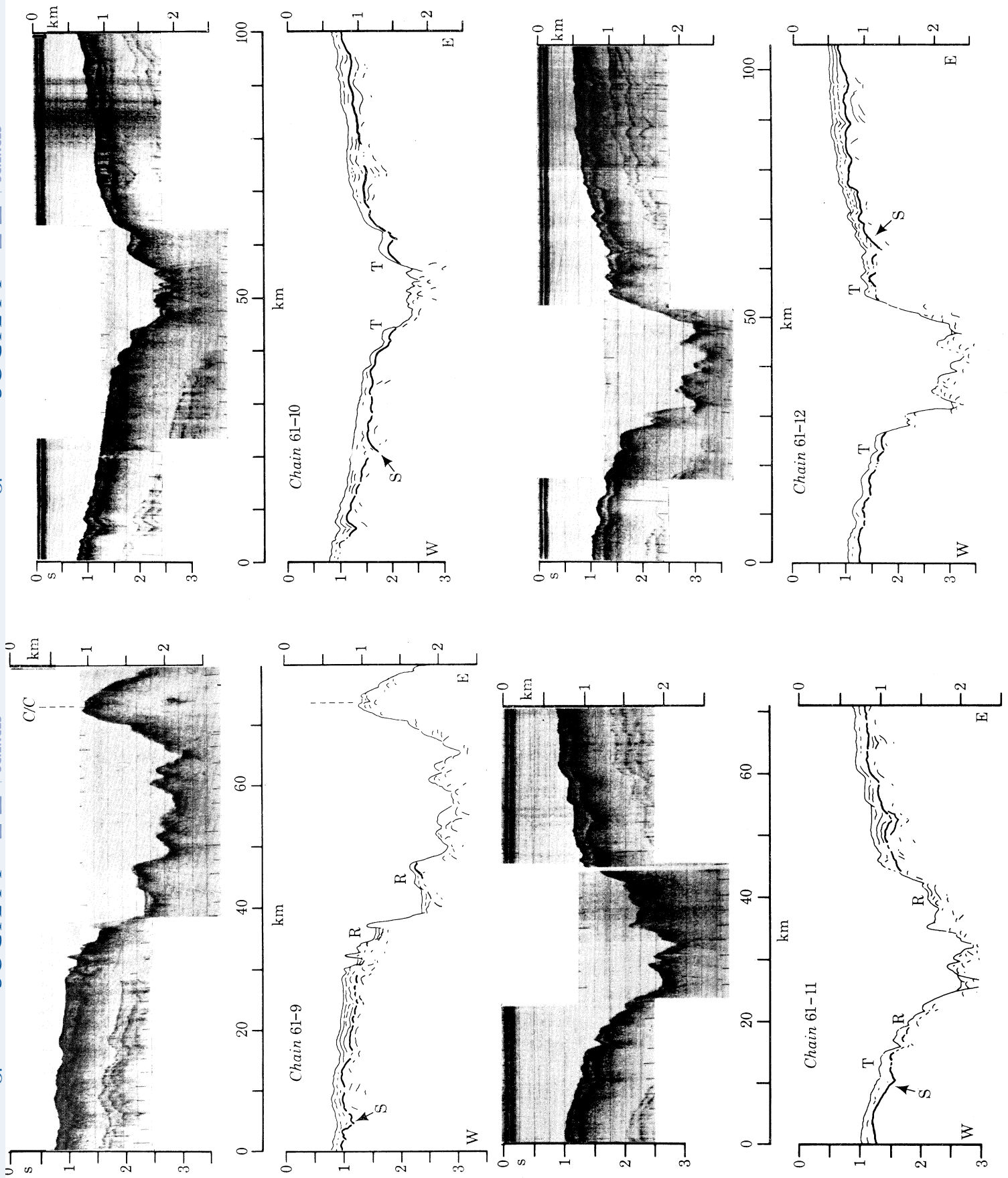


FIGURE 12

For legends see p. 146.

FIGURE 13

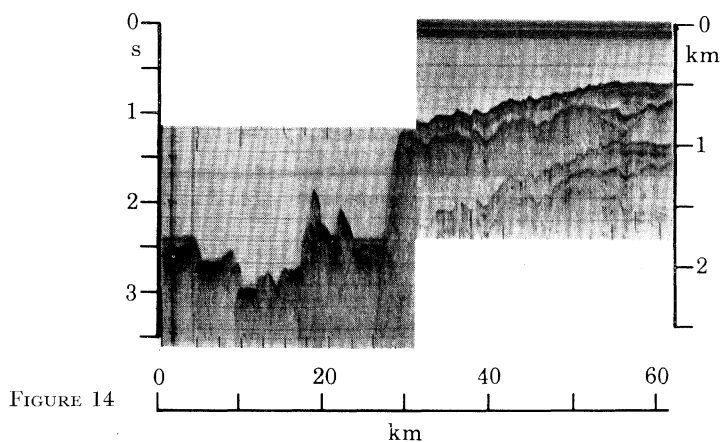


FIGURE 14

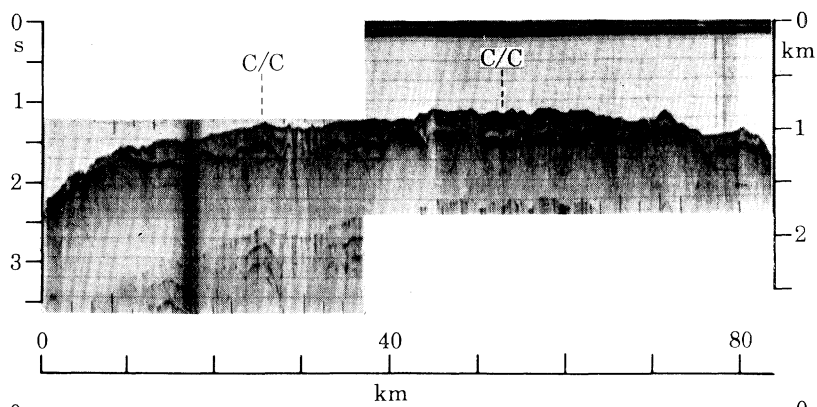
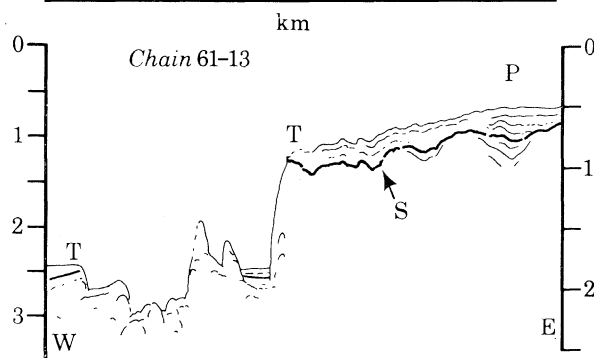
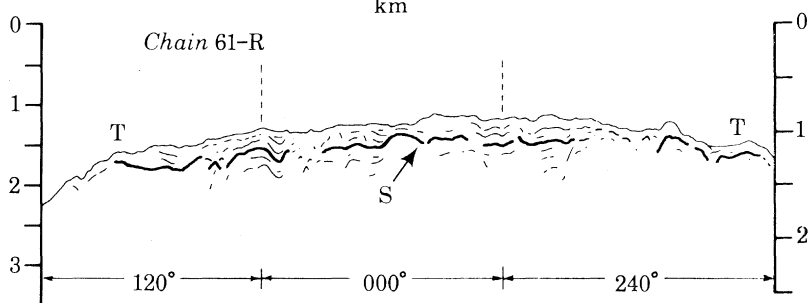


FIGURE 15
(after Ross *et al.* 1969)



For legends see p. 146.

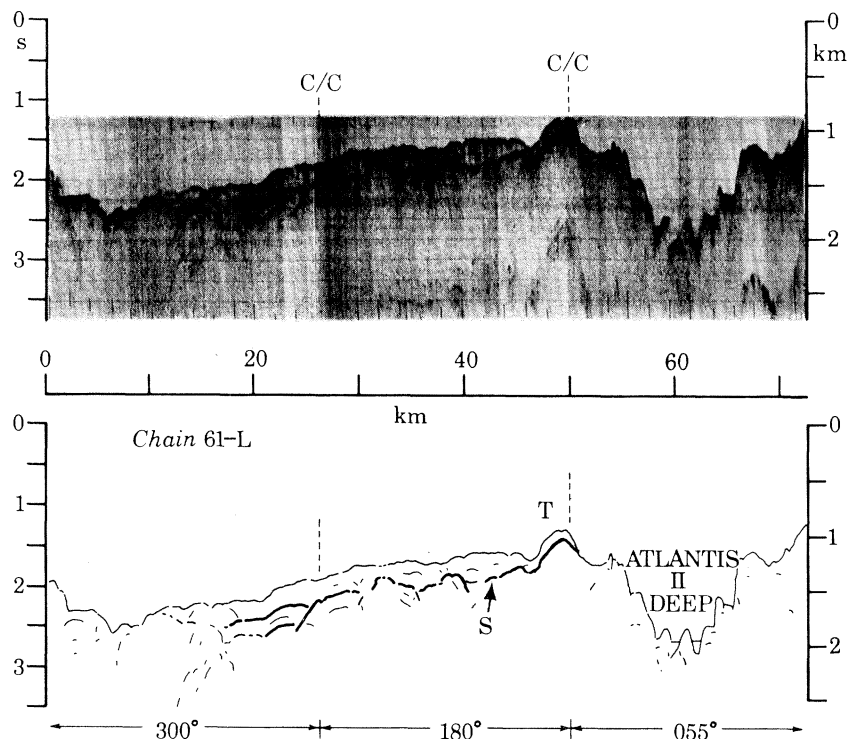
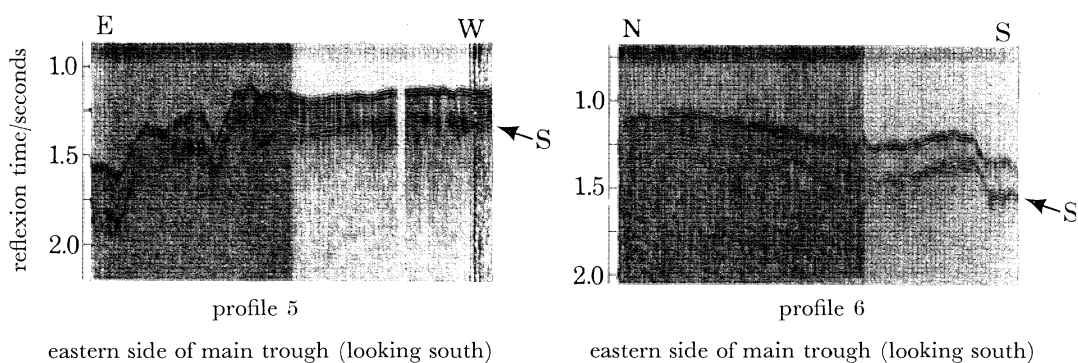
FIGURE 16 (after Ross *et al.* 1969). For legend see p. 146.

FIGURE 19. Photographs of selected *Chain 43* seismic reflexion records across the transitional region between the main trough and the axial trough near 24° N latitude (*a*) and 27° N latitude (*b*). The axial trough is toward the right and left margins of the figure. Note that the configuration of reflector S appears to shape the seafloor in the axial trough whereas in the main trough (centre of figure) the rugged nature of reflector S is not seen in the seafloor topography. Also the lack of internal reflectors in the material above reflector S near the axial trough demonstrates the relative transparency of this material as compared to that of the adjacent layered sequences in the main trough.

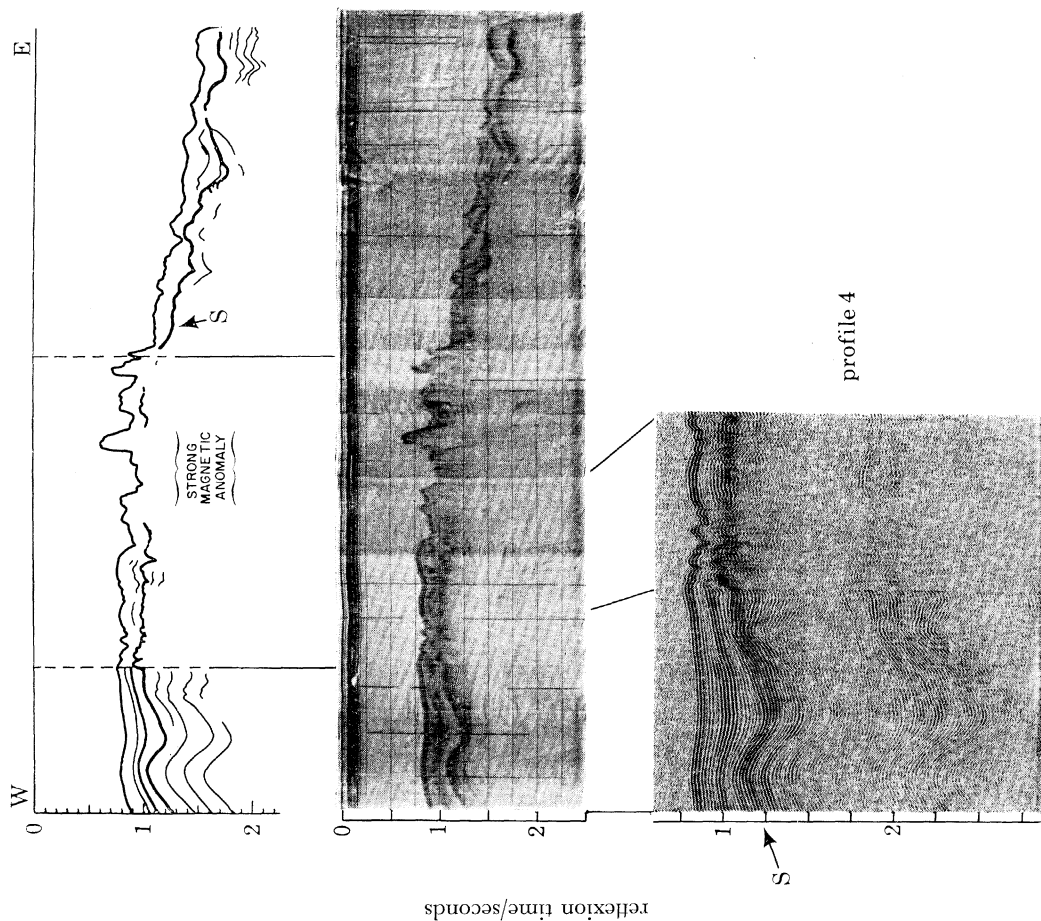


FIGURE 17. Western part of seismic profile 4 of Chain Cruise 43: (top) line drawing interpretation; (middle) seismic reflexion record, recording bandwidth 37.5 to 300 Hz; (bottom) section of reflexion record, recording bandwidth 37.5 to 75 Hz. (After Knott *et al.* 1966, figure 2.)

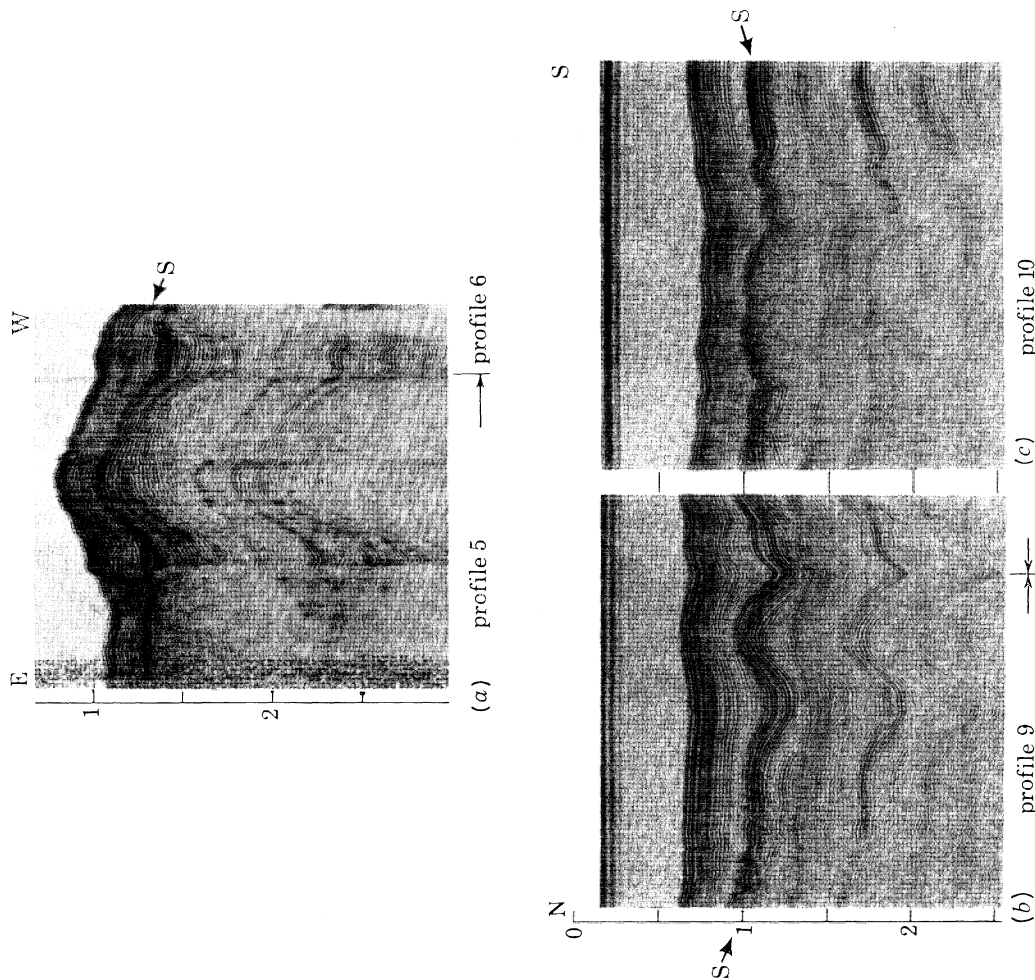


FIGURE 18. Photographs of selected Chain Cruise 43 reflexion records. (a) Western margin of the main trough at 24° N latitude. The anticline appears to be bounded by a steeply dipping fault along its north side (left) which does not involve the layers above reflector S. (b) and (c) show the western margin of the main trough near 18° N latitude. Note that reflector S appears to be more strongly folded than the sediment layers directly beneath the seafloor to profile 9. In each of these profiles, reflector S, 0.25 to 0.50 s below the seafloor, is believed to be the Miocene contact (after Knott *et al.* 1966).

a succession of upper middle Miocene evaporites and limestone (Said 1962, pp. 118–119, 192–194; Sestine 1965). Pliocene and Pleistocene material consisting of clastic sediments and reef limestones overlie the evaporites. Recently Davies & Tramontini (this volume, p. 181) have proposed that these evaporite layers probably extend to the coastal shelf off Arabia in the central Red Sea and are underlain by a basaltic layer ‘similar to the oceanic basaltic layer’.

Knott *et al.* (1966) first noted that the thickness of the post-Miocene sediments (*ca.* 400 m) on the Egyptian margin of the Red Sea is similar to the thickness of the materials above the strong reflector S and to that of the unconsolidated material observed in seismic refraction profiles. The more recent borehole data and refraction information confirm this observation. Knott *et al.* postulated that reflector S represents a discontinuity, and in some places an angular unconformity that has resulted from changes in the environment of sediment deposition at the close of Miocene time. This hypothesis is most reasonable when the distribution of reflector S (figure 21) is considered in terms of seafloor spreading in the Red Sea.

On the assumption that this reflector was both horizontal and continuous across the main trough before the formation of the axial rift zone, and that its deformation resulted from the initial phases of spreading, estimates of seafloor spreading rates can be made provided the separation direction and initial time of separation are known. Comparison of these rates with those determined from seafloor spreading magnetic models should allow an independent test of this hypothesis. Unfortunately independent and unambiguous information about the direction and age of initial spreading are not available at this time. For example, Phillips (this volume, p. 205) has shown from seafloor spreading interpretations of the magnetic anomalies in the axial trough that separation directions of N 10° E or N 60° E are possible. Reconstructions of the geologic structures across the Red Sea suggest a nearly N–S separation (Abdel-Gawad 1969 and this volume, p. 23; Girdler 1966). However, Girdler (1969) suggests that a NE–SW separation is also reasonable for certain geologic reconstructions. First motion slip vector directions for earthquakes in the axial trough near 21 and 17° N latitude support a N 40° E to N 60° E separation direction (Fairhead & Girdler, this volume, p. 49; Sykes 1968). Clearly more detailed study is required before a firm conclusion can be drawn as to the true spreading direction.

Representative distances for a N 10° E separation direction are shown in figure 21 (block numbers) for the purposes of illustration. The average distance is 74 km. The inferred minimum spreading rate based on separation immediately after formation of the late Miocene discontinuity (say 5 to 6 Ma ago) is 0.7 cm a⁻¹. Alternatively, if the separation direction were in a more NE direction (say N 60° E) as suggested by the magnetic trend and earthquake first motion studies, a separation distance of 48 km would indicate a rate of 0.44 cm a⁻¹.

Whether separation began in late Miocene time is problematic. The deformation of the Miocene evaporites, concomitant with the initiation of spreading, clearly suggest at least a post-Miocene age. How much younger is difficult to determine. The fact that not all the overlying Plio-Pleistocene clastics are deformed with the evaporites along the margins of the main trough argues that initial separation may have begun after deposition of some of the basal Pliocene sediments, but before the bulk of the post-Miocene sediments (those above reflector S) were laid down. In the axial region all the post-Miocene sediments are deformed because tectonism has probably been continuously active here since the initial rifting. A more precise age other than Pliocene for the sediments immediately above the evaporites is not available. In any event, a late Miocene–early Pliocene initiation time and a 74 km separation

distance provides a rate in good agreement with spreading rates along the Dead Sea rift determined independently by Freund *et al.* (1968). From observations of a 40 to 45 km displacement (inferred to be half the separation distance) of certain late Miocene–early Pliocene river beds, sedimentary deposits, and volcanic bodies they calculated a minimum spreading rate of 0.35 cm a^{-1} , based on a date of 12 Ma for the Miocene/Pliocene boundary. However, recent work by Berggren (1969) has shown that the Plio-Miocene boundary is probably only about 6 Ma old. Thus the rate of Freund *et al.* would be about 0.7 cm a^{-1} .

Although this rate compares reasonably well with the 1.0 to 1.6 cm a^{-1} rate inferred from the magnetic profiles (Phillips, this volume, p. 205; Vine 1966) two further factors must be considered before we can evaluate the apparent agreement of these values. First, it is not clear if the 45 km displacement along the Dead Sea rift is exactly one half the separation distance for the motion of the African and Arabian crustal plates. The fact that the rift does not extend southward into Africa across the main trough of the Red Sea, presumably the axis of opening (spreading), makes it likely that the displacement represents the total separation. Clearly, north and south displacements of 45 km from a stationary axis would require motion of both the African and Arabian plates relative to a third plate consisting of northernmost Egypt, Sinai and Israel. There is little evidence for major horizontal displacements here. Alternatively, the spreading axis could simply migrate northward away from an African plate which includes Sinai and Israel. In this case the 45 km Dead Sea displacement would reflect the total opening during the last 6 Ma. The latter explanation seems more reasonable. This suggests the rate of Freund *et al.* should indeed be 0.35 cm a^{-1} ; they seem to have deduced the correct rate for the wrong reasons. Secondly, if the pole of rotation for the separation of Arabia and Africa (Morgan 1968) is located north and west of the Red Sea–Dead Sea region as McKenzie (this volume, p. 393). As Le Pichon & Heirtzler (1968) and Girdler (1966) propose, the spreading rate in the southern Red Sea may be somewhat larger than in the Dead Sea region. Freund *et al.* recognized this possibility and contended on the basis of Girdler's (1966) proposed rotation scheme that the rate in the Red Sea should be twice as high as along the Dead Sea rift. Since their 0.35 cm a^{-1} rate is precisely half the 0.7 cm a^{-1} rate estimated from the reflector S separation distance, this estimate is considered reasonable for the minimum spreading rate in the southern Red Sea.

It should be emphasized that seafloor spreading interpretations of magnetic anomaly profiles across the axial trough (Phillips, this volume, p. 205; Girdler 1968; Vine 1966) imply that the present phase of spreading has been active only for the last 3 Ma. Thus, since the anomaly features characteristic of this time interval span the entire axial trough, it appears that the trough cannot be much older than 3 Ma (Late Pliocene). If this is true the spreading rate inferred from the Dead Sea rift displacement and reflector S separation distance across the axial trough should be about 1.4 cm a^{-1} . This rate is in close agreement with the 1.6 cm a^{-1} rate inferred directly from the marine magnetic profiles for a $\text{N } 10^\circ \text{ E}$ separation direction. Further, a $\text{N } 60^\circ \text{ E}$ separation direction provides a rate of about 0.9 cm a^{-1} . This rate is in even better agreement with the 1.0 cm a^{-1} rate determined from the magnetic profiles commensurate with a $\text{N } 60^\circ \text{ E}$ spreading direction (Phillips this volume, p. 205; Vine 1966). A late Pliocene initiation of spreading in the axial trough is also supported by the reflexion information which suggests that basal Pliocene sediments above reflector S were deformed with reflector S at the initiation of spreading.

Another aspect of our seismic reflexion information relevant to a spreading hypothesis for

the Red Sea axial trough concerns the thickness of the relatively transparent layer that extends from the seaward margins of the main trough down the flanks of the axial trough. A gradual increase in thickness of this layer outward from the centre of the axial trough is clearly shown in figures 11 to 16. The layered sequences on the margins of the main trough appear essentially uniform in thickness. To account for these differences in thickness it is reasonable to propose that the transparent layer has been deposited on newly exposed materials brought to the surface successively as spreading proceeded. Whether this material is older evaporites or new oceanic type materials is unknown. The fact that the configuration of the transparent layer reflects more faithfully the topography of the underlying material as the axial trough is approached further argues that the transparent layer and underlying opaque material were formed more recently than the materials along the margins. Similar evidence showing a progressive decrease in sediment thickness toward the Mid-Atlantic ridge has been cited by Ewing & Ewing (1967) to support seafloor spreading in the Atlantic Ocean. Evidence from our profiles could also be used to support seafloor spreading in the Red Sea axial trough. However, in view of the large errors inherent in measuring the thin sediment cover and the short distance from the locus of spreading, this apparent correlation is of limited value.

The local deformation of the sediment layers in the northern Red Sea may also be explained by seafloor spreading. For example, the many disrupted sediment sequences and deep crevasses north of 24° N latitude can be interpreted to represent sections across strike-slip fault planes. The crevassed regions particularly suggest severe recent deformation involving the seafloor. The close similarity in character of these disturbed sections is illustrated in figure 20. The locations of certain of these sections have been plotted in figure 21 and an attempt has been made to correlate them across the region. Although other correlations are possible because of the limited areal coverage, those shown by the connecting lines can be inferred to result from motions parallel to many local strike-slip faults. These directions of motion appear to be consistent with the direction of true spreading inferred from magnetic anomalies (Phillips, this volume, p. 205) and the trend of the Dead Sea–Aqaba rift.

SUMMARY AND CONCLUSIONS

Continuous seismic profiles have been used to map the geographic distribution of the strong subbottom reflector S and to infer the geologic history of the deformed layered materials beneath the Red Sea. This information can be used to estimate the age for the initial formation of the axial trough. Specifically, if reflector S represents a discontinuity after deposition of Late Miocene evaporites and limestones and its deformation marks the initiation of seafloor spreading in the axial trough, the following observations lead to the tentative conclusion that the axial trough has formed since late Miocene time and in all probability within the last 2 to 3 Ma.

(1) The subbottom reflector S is not found in the axial trough or central part of the Red Sea south of 25° N latitude. Where it is present along the margins, it is mildly folded and faulted; the overlying Plio-Pleistocene layers are largely undeformed. This suggests that the separation (spreading) started before deposition of the bulk of the overlying sediments.

(2) The approximate separation distance of reflector S across the axial trough in the range of probable spreading directions (N 10° E to N 60° E) is 74 to 48 km. This requires a minimum spreading rate of 0.4 to 0.7 cm a⁻¹, assuming the initiation of spreading 5.5 Ma ago immediately after the disconformity represented by reflector S developed.

(3) However, the fact that not all the Plio-Pleistocene sediments above reflector S in the margins of the main trough are undeformed implies initial rifting may have begun after deposition of certain of these sediments. Also a seafloor spreading interpretation of the magnetic anomalies which occupy the entire axial trough further suggests spreading has been active here only during the last 2–3 Ma. Applying a 2.5 Ma age for the initiation of spreading to the reflector S separation distances yields a spreading rate of 1.4 to 0.9 cm a⁻¹. These values are in better agreement with the spreading rates of 1.6 to 1.0 cm a⁻¹ inferred directly for the magnetic

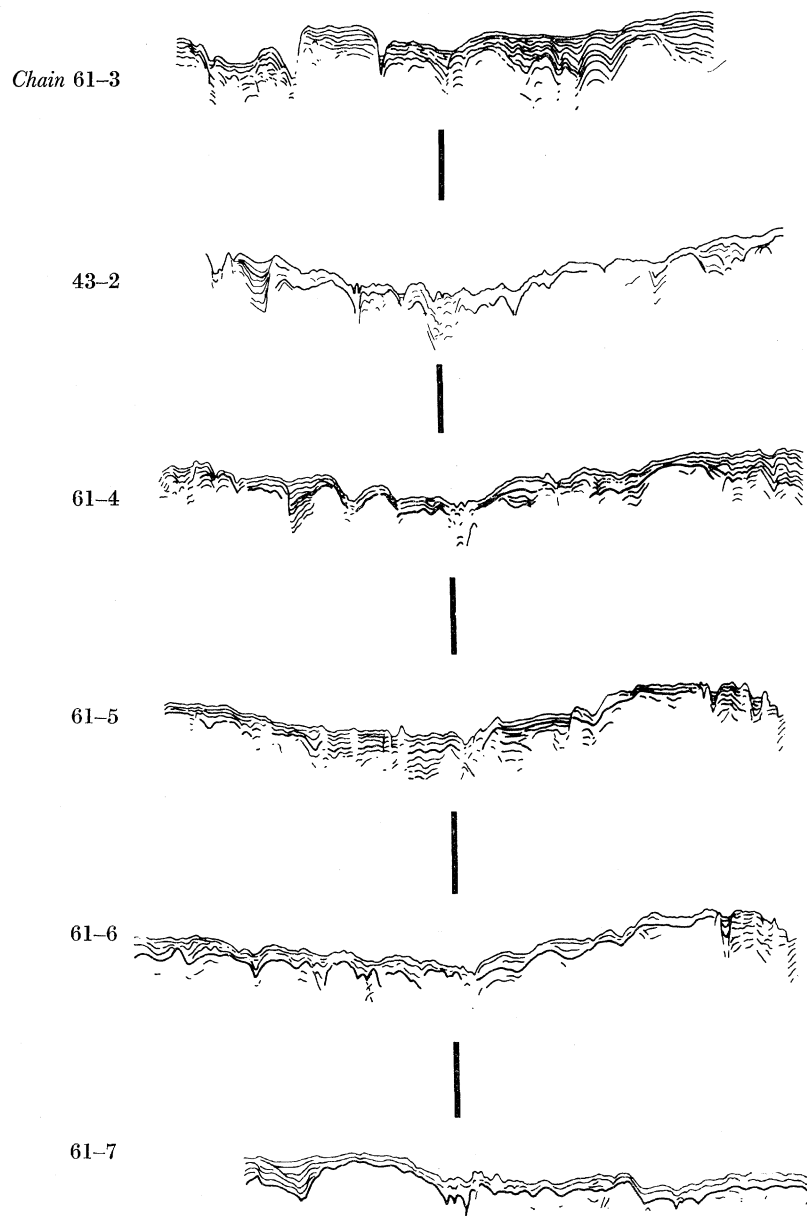


FIGURE 20. Seismic profiles in the northern Red Sea. The general nature of deformed sediment layers beneath the narrow crevassed regions of the seafloor is illustrated. The profiles have been aligned so that the vertical line connects that portion of the profiles showing striking similarities. However, it must be emphasized that since the profiles have different horizontal scales, the particular feature denoted by the vertical line cannot be interpreted to be continuous along a straight line. On the map of figure 21, this feature and certain others appear to be aligned along short offset line segments suggestive of *en échelon* strike-slip fault planes (see text).

anomaly profiles. This closer correspondence between independently determined spreading rates strongly supports the hypothesis that the axial trough began to form in Pliocene time (2 to 3 Ma ago) rather than late Miocene. Not until more precise estimates of the age of the

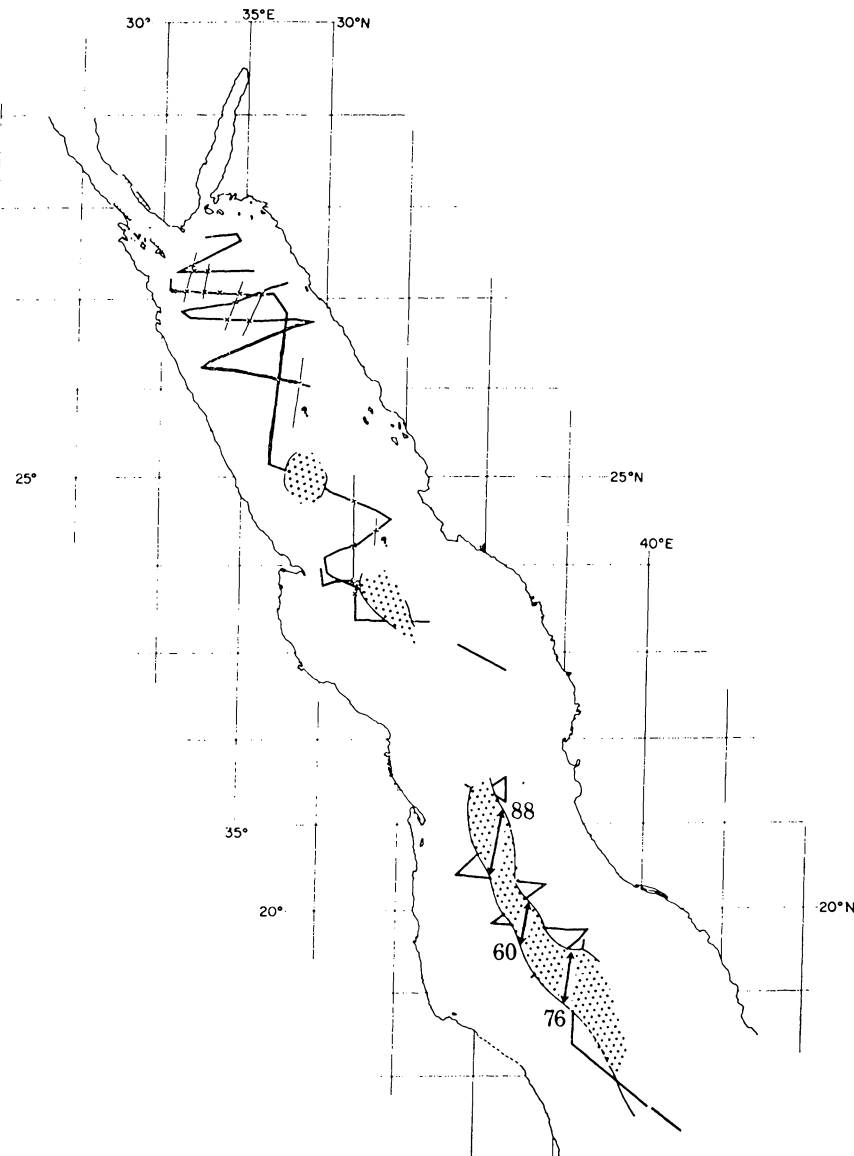


FIGURE 21. Distribution of reflector S across the main trough of the Red Sea. The solid lines show the portions of the *Chain Cruises* 43 and 61 profiles where reflector S is observed. The stippled area encloses those portions of the profiles where it is absent. Crosses show the location of strongly disturbed zones along each profile believed to be sections across strike-slip fault planes. Lines connecting the crosses show possible directions of inferred motion. Block numbers indicate representative separation distances of reflector S in kilometres across the axial trough for a N 10° E separation. For a N 60° E separation direction the distances are 57, 39 and 49 km respectively.

deformed basal Pliocene sediment above reflector S and the direction of true separation are available will it be possible to determine the spreading rate more accurately by mapping reflector S across the axial trough.

We thank Miss Elizabeth T. Bunce for many useful discussions and for critically reviewing the manuscript; E. E. Hays, and J. M. Hunt who were Chief Scientists during the *Chain* Cruise 61 and the Master, Officers, and Crew of R.V. *Chain* for their cooperation. This work was supported by the Office of Naval Research (Contracts Nonr-4029(00) NR 260-101 and N 00014-66-CO 241, NR 083-004), and the National Science Foundation (Grant GA-584).

REFERENCES (Phillips & Ross)

- Abdel-Gawad, M. 1969 Geological structures of the Red Sea area inferred from satellite pictures. In *Hot brines and recent heavy mineral deposits in the Red Sea*, pp. 25–37 (Degen, E. T. and Ross, D. A., eds). New York: Springer-Verlag.
- Berggren, W. A. 1969 Cenozoic Chrono-stratigraphy, planktonic foramineral zonation and the Radiometric timescale. *Nature, Lond.* **224**, 1072–1075.
- Degens, E. T. & Ross, D. A. 1969 (eds.) *Hot brines and recent heavy mineral deposits in the Red Sea*. New York: Springer-Verlag.
- Drake, C. L. & Girdler, R. W. 1964 A geophysical study of the Red Sea. *Geophys. J. R. Astr. Soc.* **8** (5), 473–495.
- Ewing, J. & Ewing, M. 1967 Sediment distribution of the mid-ocean ridges with respect to spreading of the seafloor. *Science, N.Y.* **156**, 1590–1592.
- Freund, R., Zak, I. & Garfunkel, Z. 1968 Age and rate of the sinistral movement along the Dead Sea Rift. *Nature, Lond.* **220**, 253–255.
- Girdler, R. W. 1958 The relationship of the Red Sea to the East African rift system. *Q. Jl geol. Soc. Lond.* **114**, 79–105.
- Girdler, R. W. 1963 Geophysical studies of rift valleys, in *Phys. Chem. Earth* **5**, 121–156.
- Girdler, R. W. 1966 The role of translational and rotational movements in the formation of the Red Sea and Gulf of Aden. In *The World Rift System. Geol. Survey of Canada, Paper 66–14*, 65–77.
- Girdler, R. W. 1969 The Red Sea—a geophysical background. In *Hot brines and recent heavy mineral deposits in the Red Sea*, pp. 38–58 (Degen, E. T. and Ross, D. A., eds). New York: Springer-Verlag.
- Knott, S. T., Bunce, E. T. & Chase, R. L. 1966 Red Sea seismic reflection studies. In *The World Rift System, Geol. Survey of Canada, Paper 66–14*, 33–61.
- Laughton, A. 1966 The Gulf of Aden, in relation to the Red Sea and the Afar depression of Ethiopia. In *The World Rift System, Geol. Survey of Canada, Paper 66–14*, 78–97.
- LePichon, X. & Heirtzler, J. R. 1968 Magnetic anomalies in the Indian Ocean and seafloor spreading. *J. geophys. Res.* **73**, 2101–2118.
- Phillips, J. D., Woodside, J. & Bowin, C. O. 1969 Magnetic and gravity anomalies in the central Red Sea. In *Hot brines and recent heavy mineral deposits in the Red Sea*, pp. 98–113 (Degen, E. T. and Ross, D. A., eds). New York: Springer-Verlag.
- Quennell, A. M. 1958 The structural and geomorphic evolution of the Dead Sea Rift. *Q. Jl geol. Soc. Lond.* **114**, 1–24.
- Ross, D. A., Hays, E. E. & Allstrom, F. C. 1969 Bathymetry and continuous seismic profiles of the hot brine region of the Red Sea. In *Hot brines and recent heavy metal deposits in the Red Sea*, pp. 82–97 (Degen, E. T. and Ross, D. A., eds). New York: Springer-Verlag.
- Said, R. 1962 *The geology of Egypt*. New York: Elsevier.
- Sestine, J. 1965 Cenozoic stratigraphy and depositional history, Red Sea coast, Sudan. *Bull. Am. Ass. Petrol. Geol.* **49**, 1453–1472.
- Swartz, D. H. & Arden, D. D. 1960 Geologic history of Red Sea area. *Bull. Am. Ass. Petrol. Geol.* **44**, 1621–1637.
- Sykes, L. 1968 Seismological evidence for transform faults, seafloor spreading and continental drift. In *The history of the Earth's crust*, pp. 120–150 (Phinney, R. A., ed.). Princeton University Press.
- Vine, F. J. 1966 Spreading of the seafloor. New evidence. *Science, N.Y.* **154**, 1405–1415.

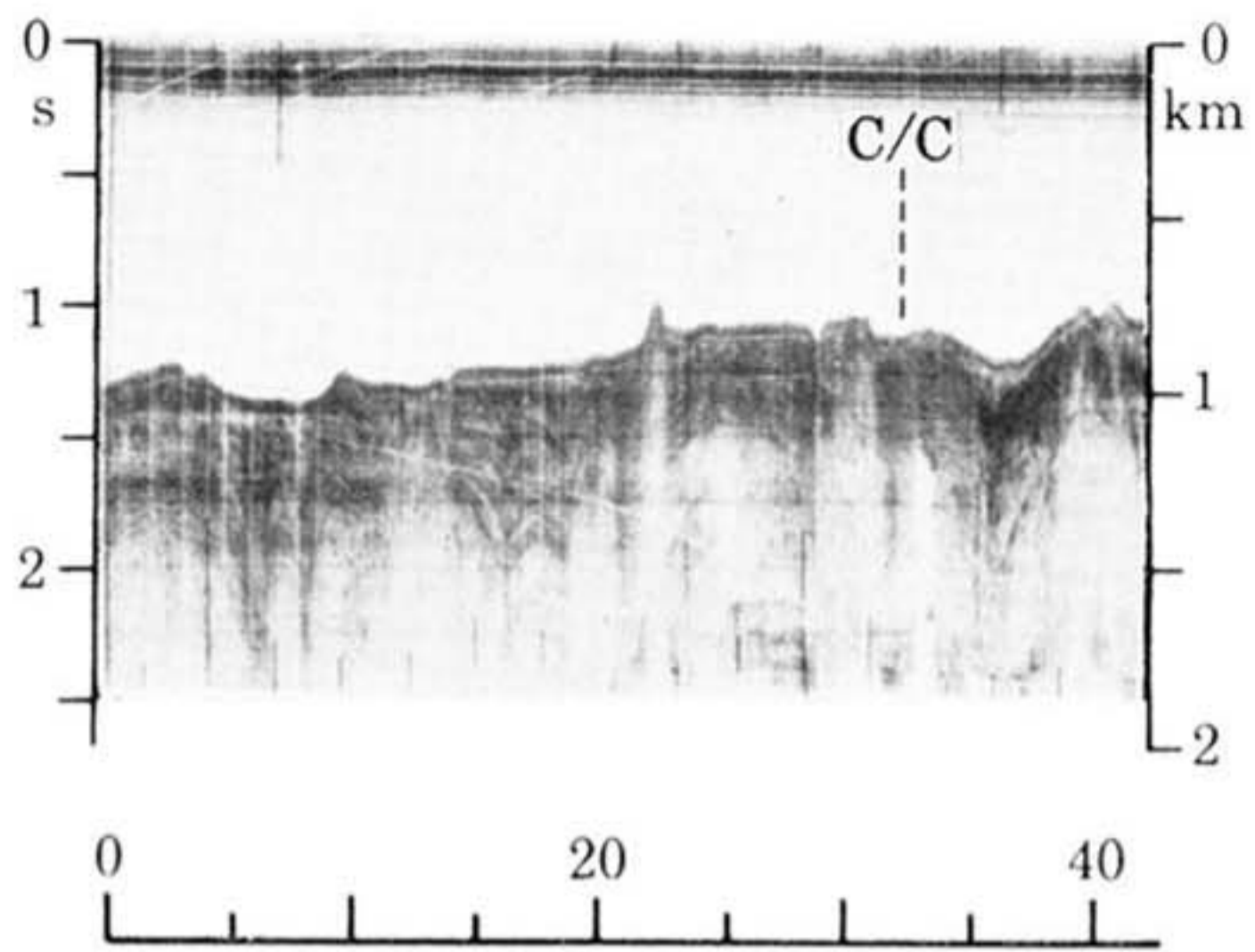


FIGURE 2

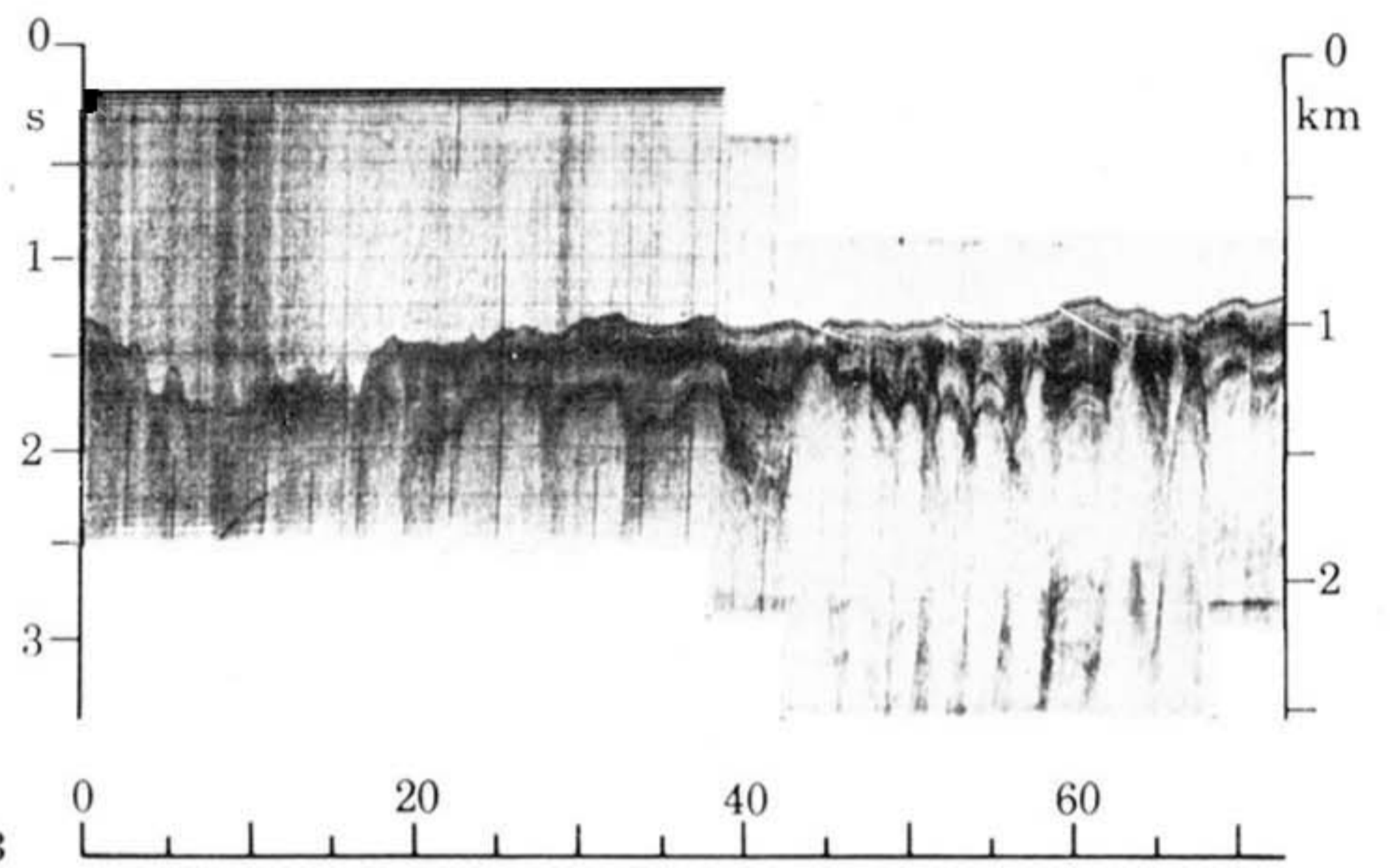


FIGURE 3

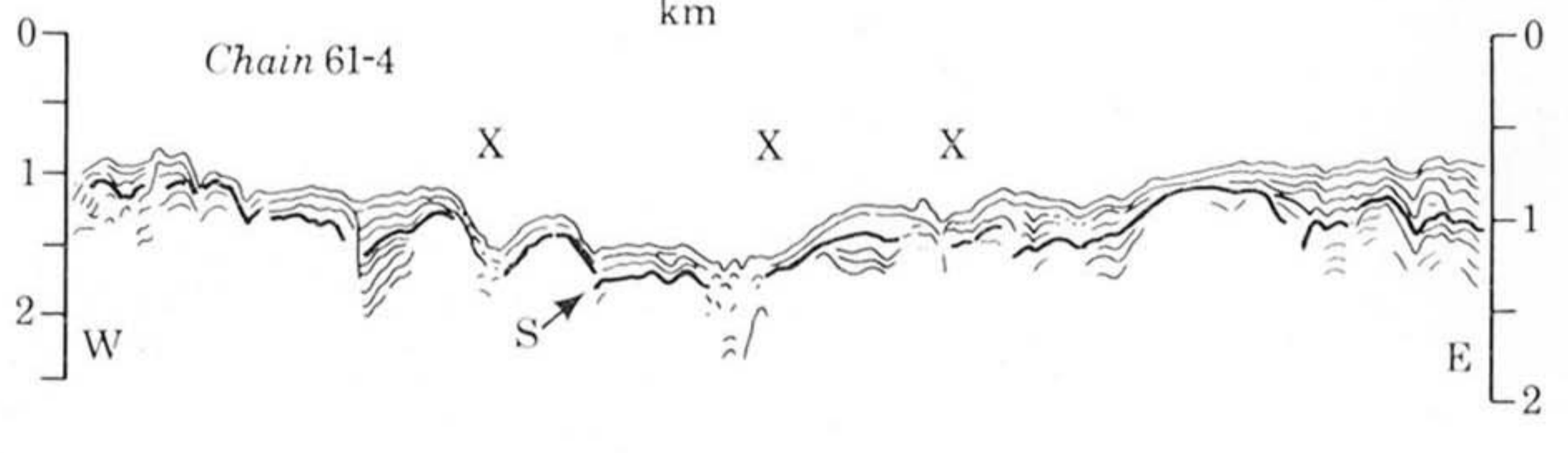
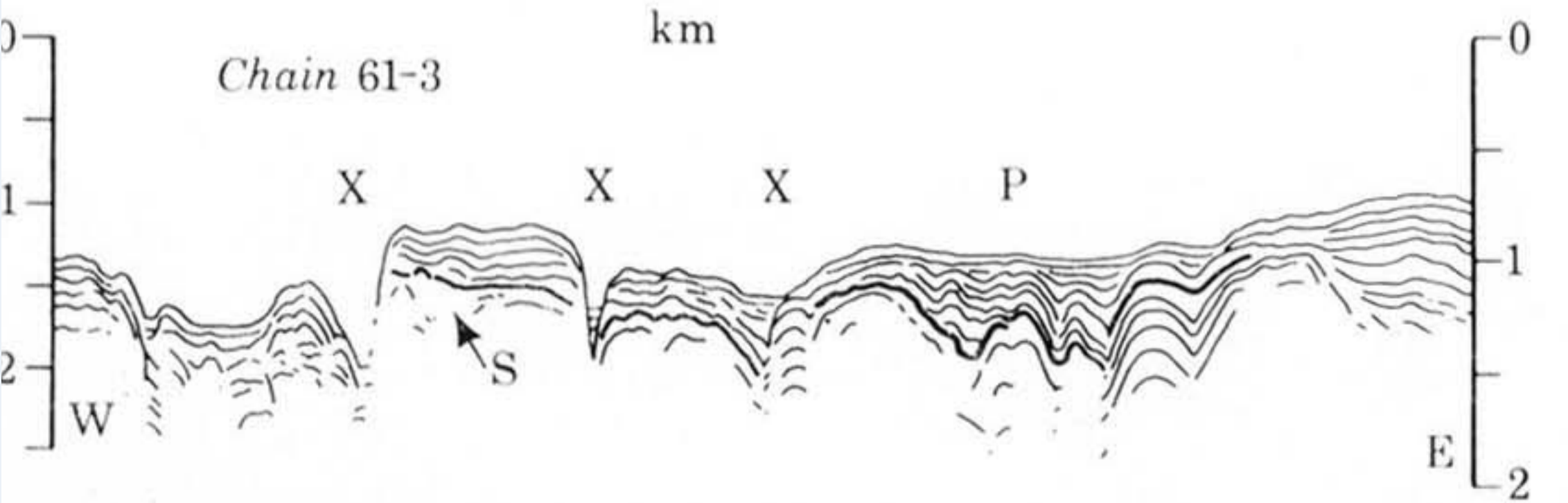
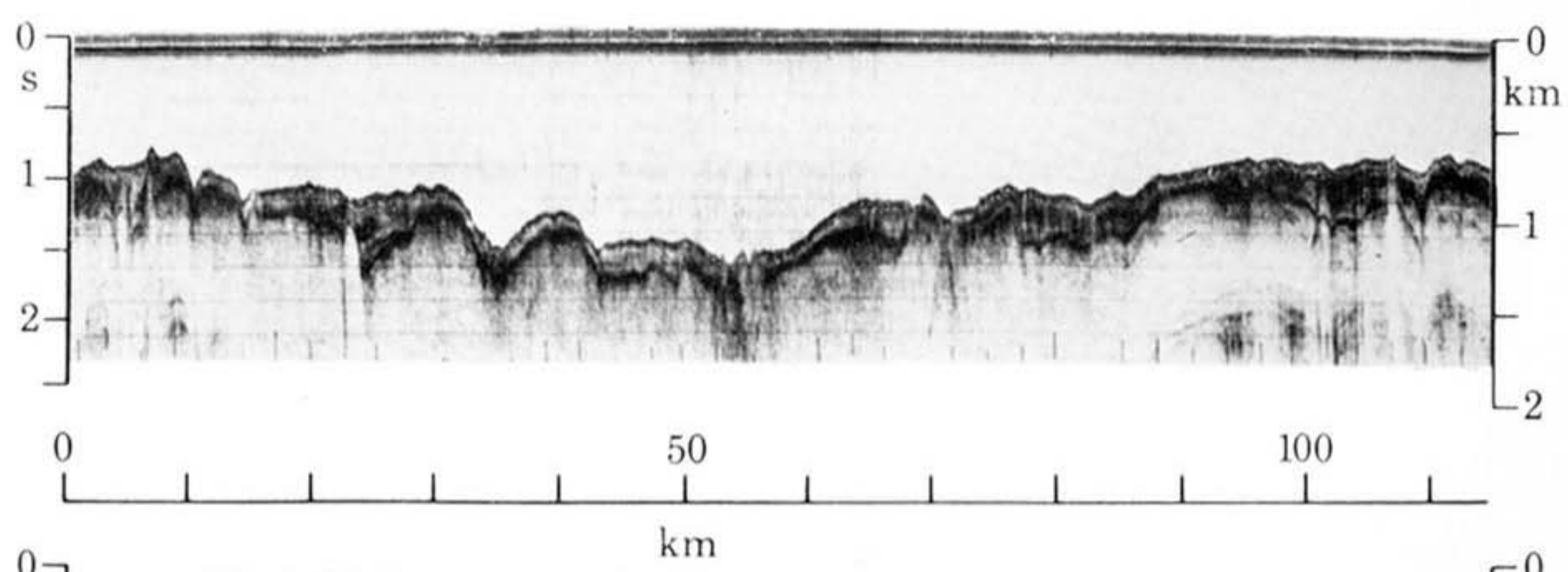
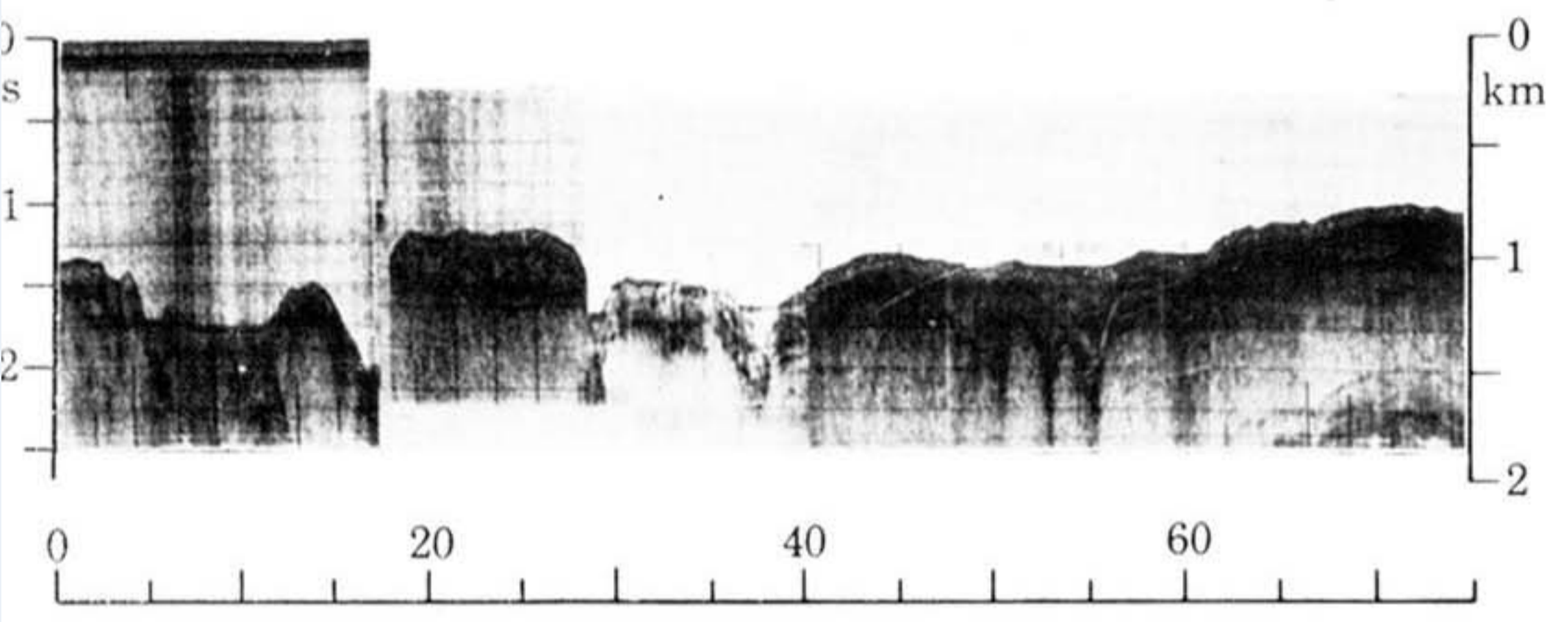
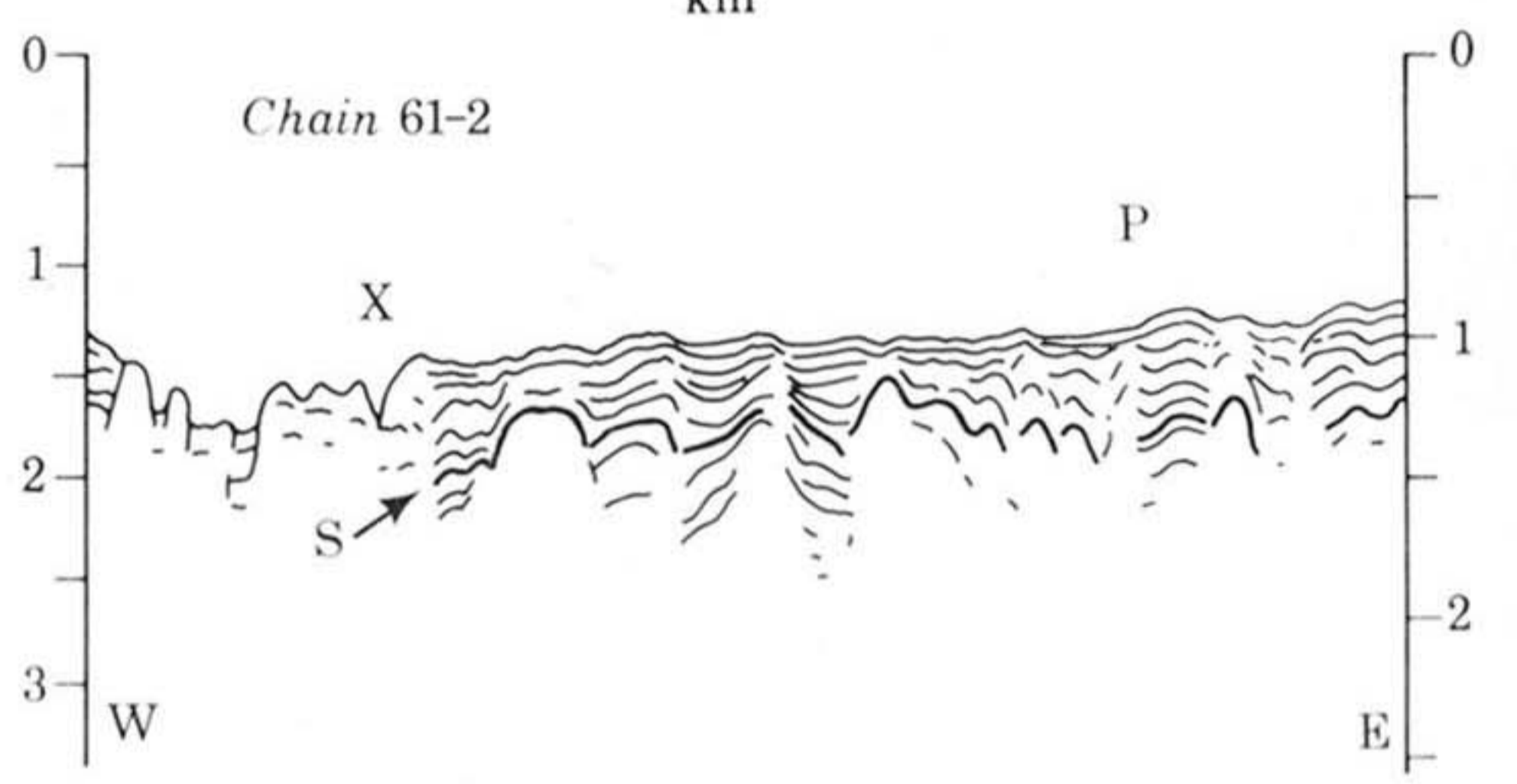
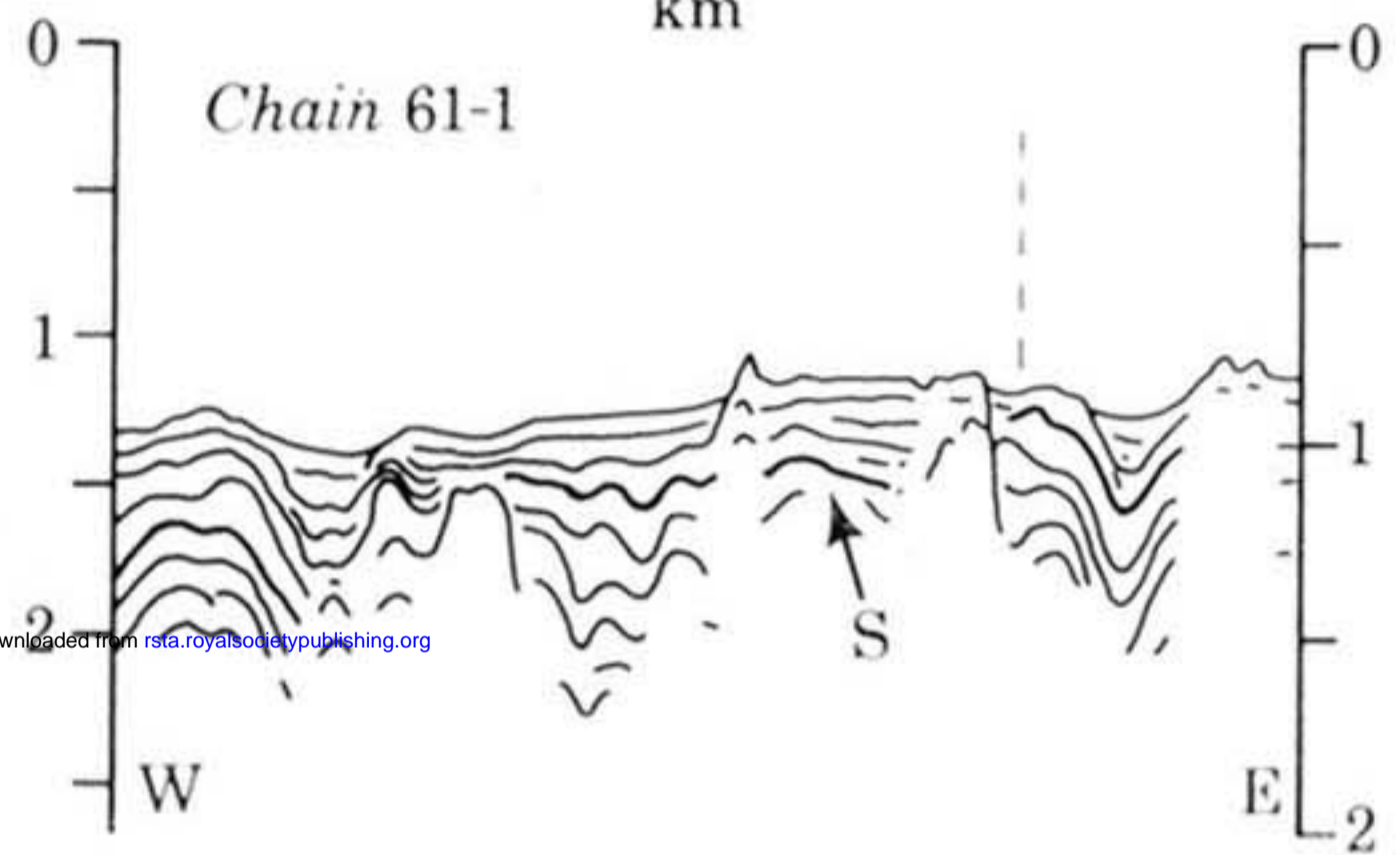


FIGURE 4

For legends see facing page.

FIGURE 5

FIGURE 6

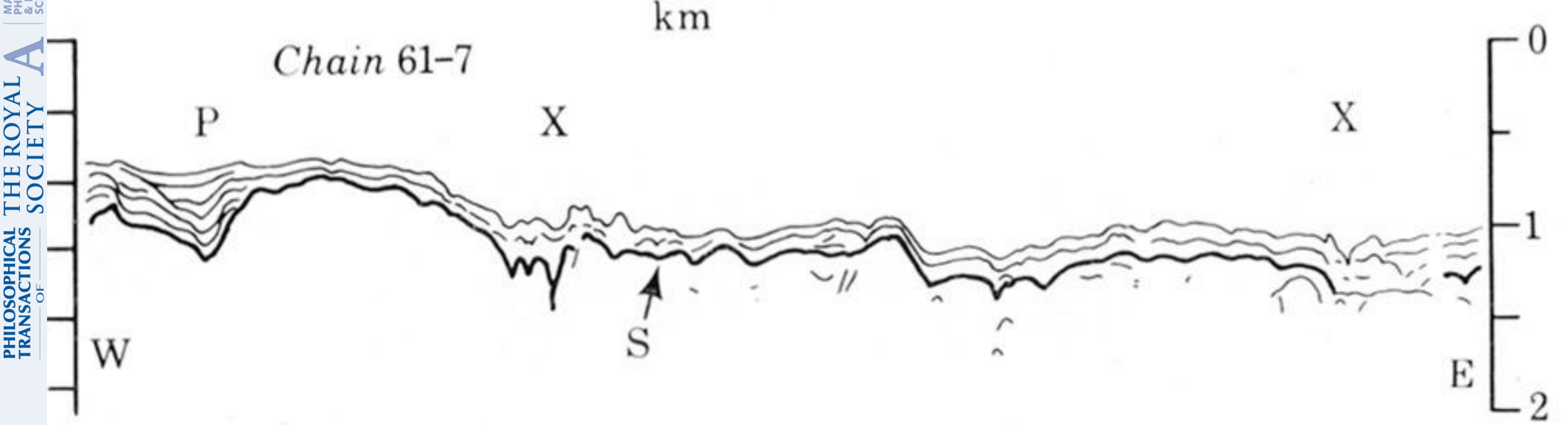
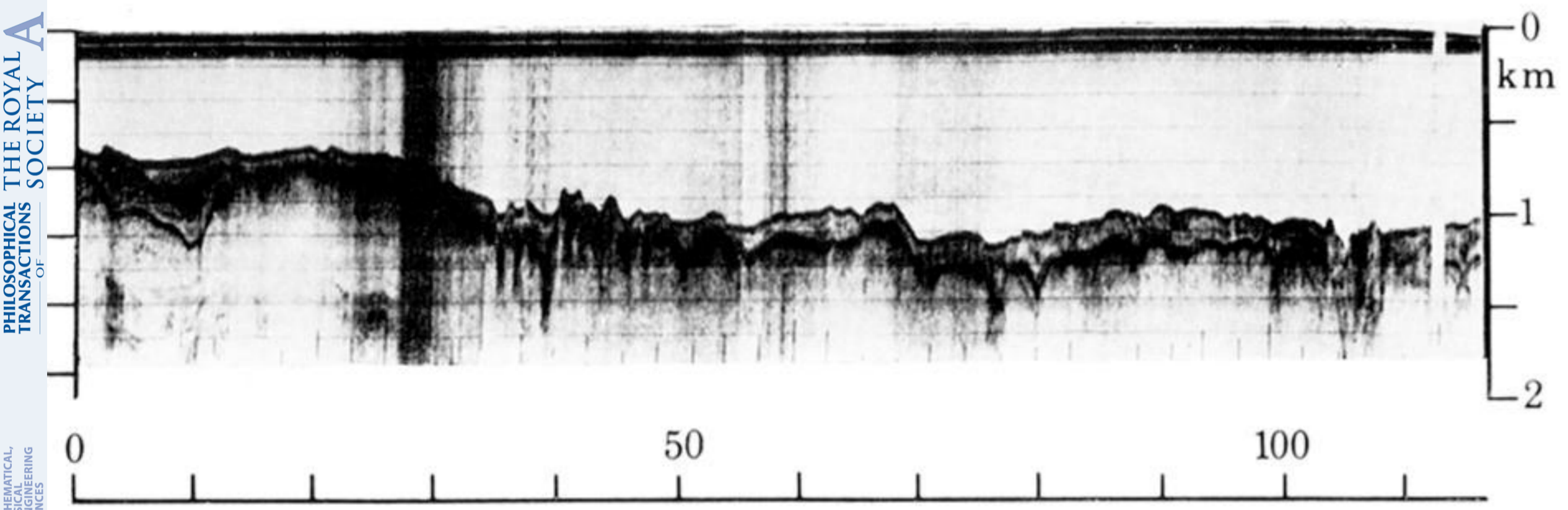
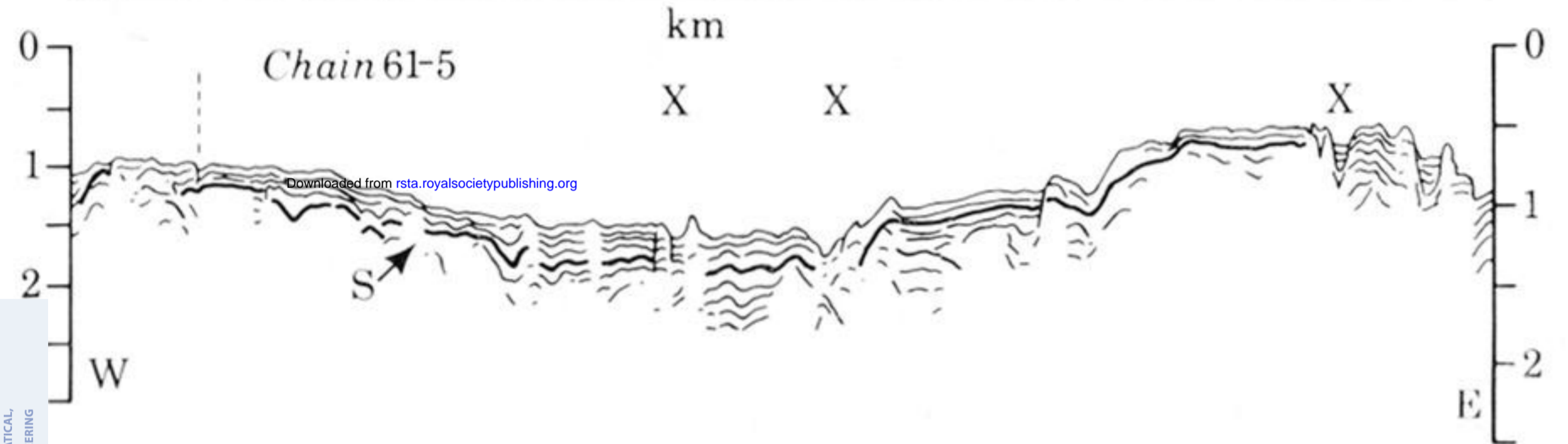
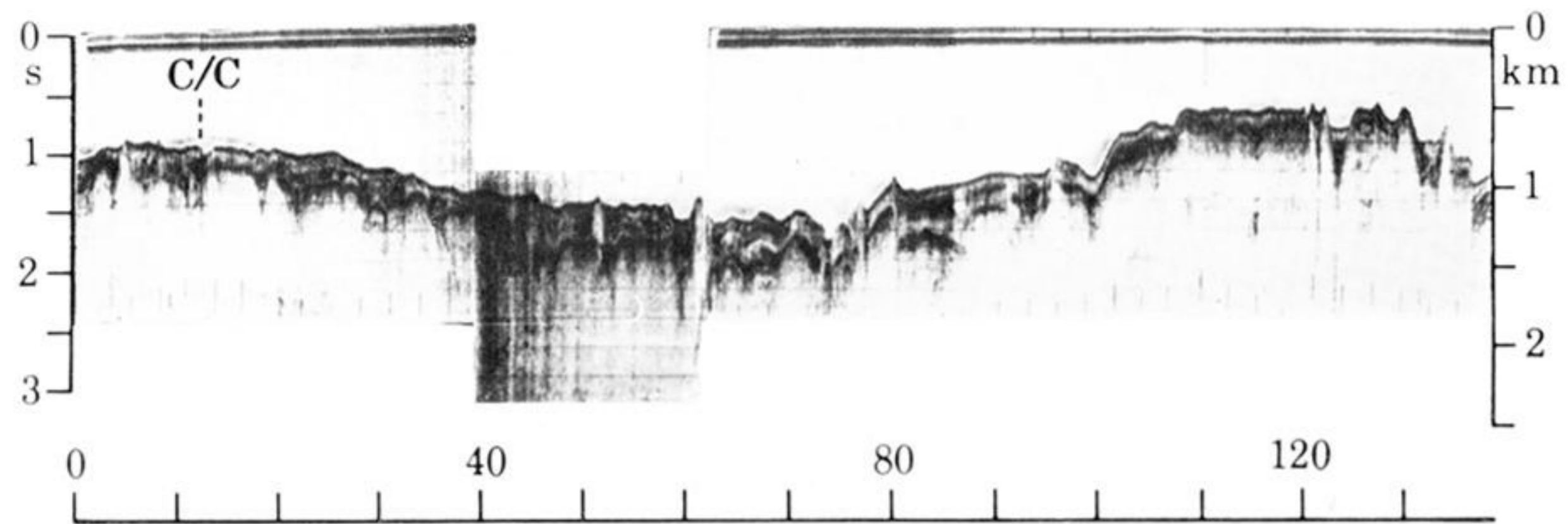


FIGURE 8

FIGURE 7

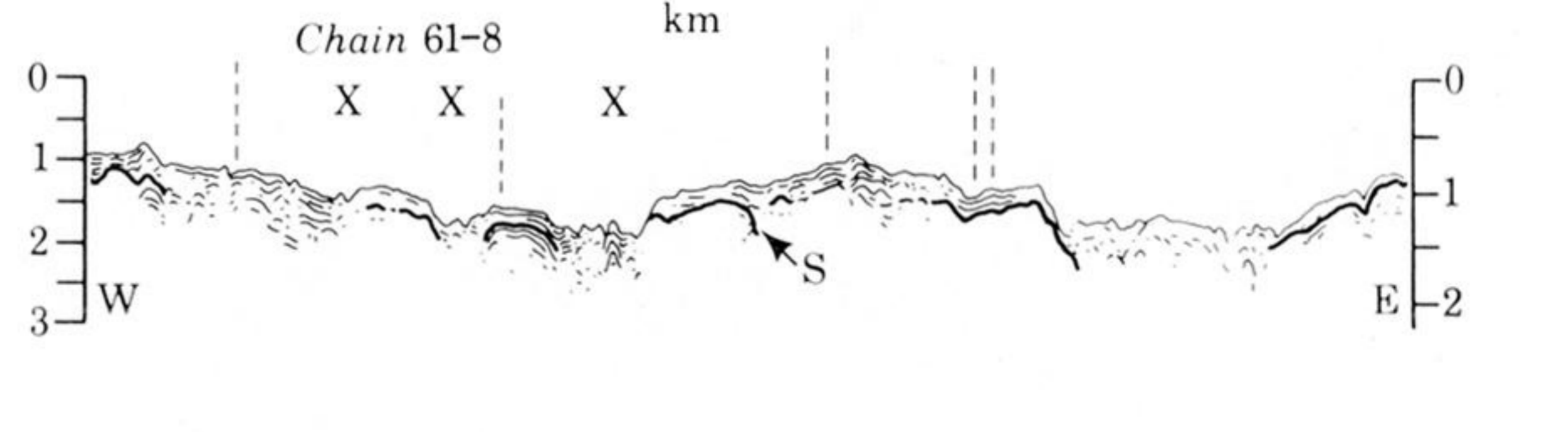
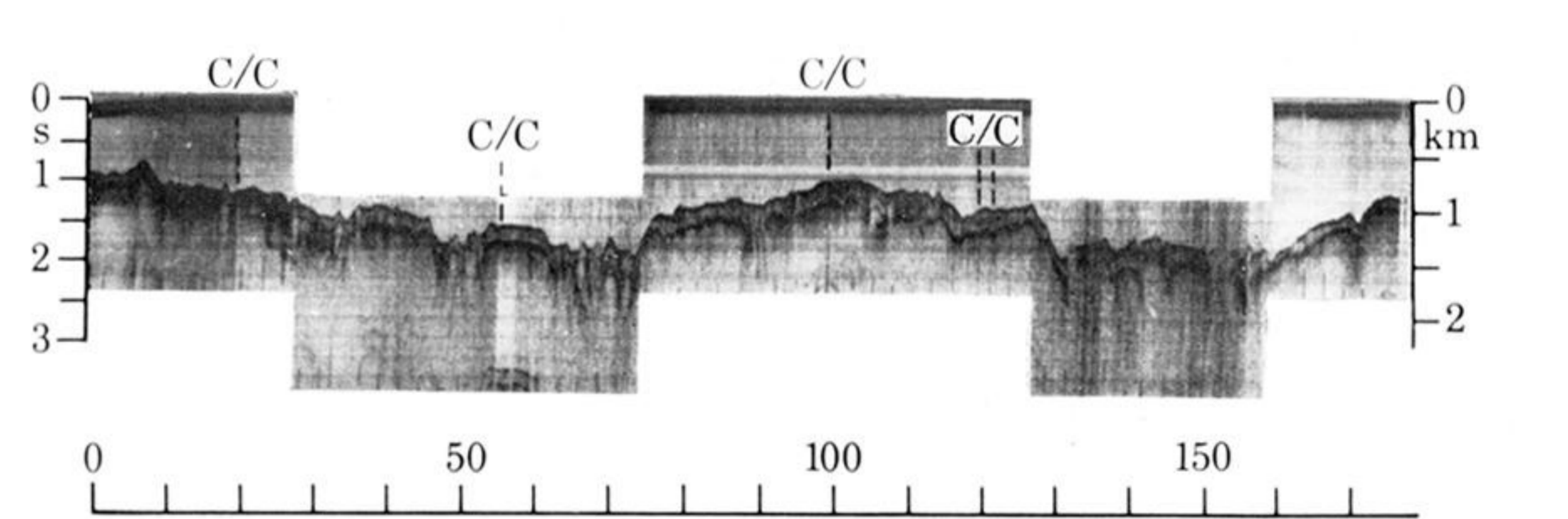
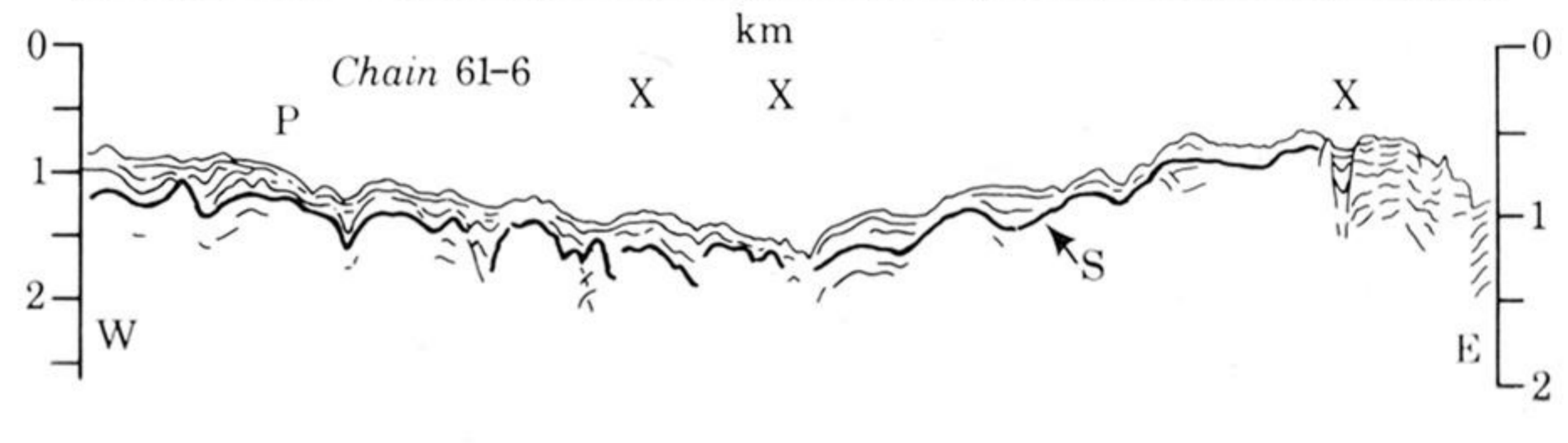
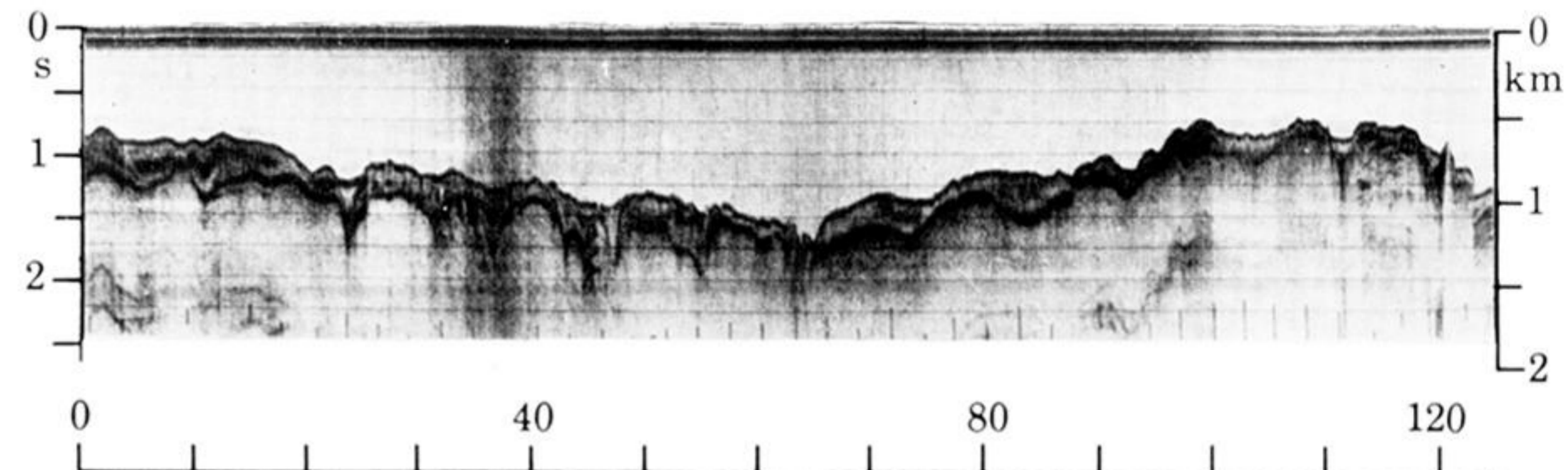


FIGURE 9

For legends see p. 146.

FIGURE 10

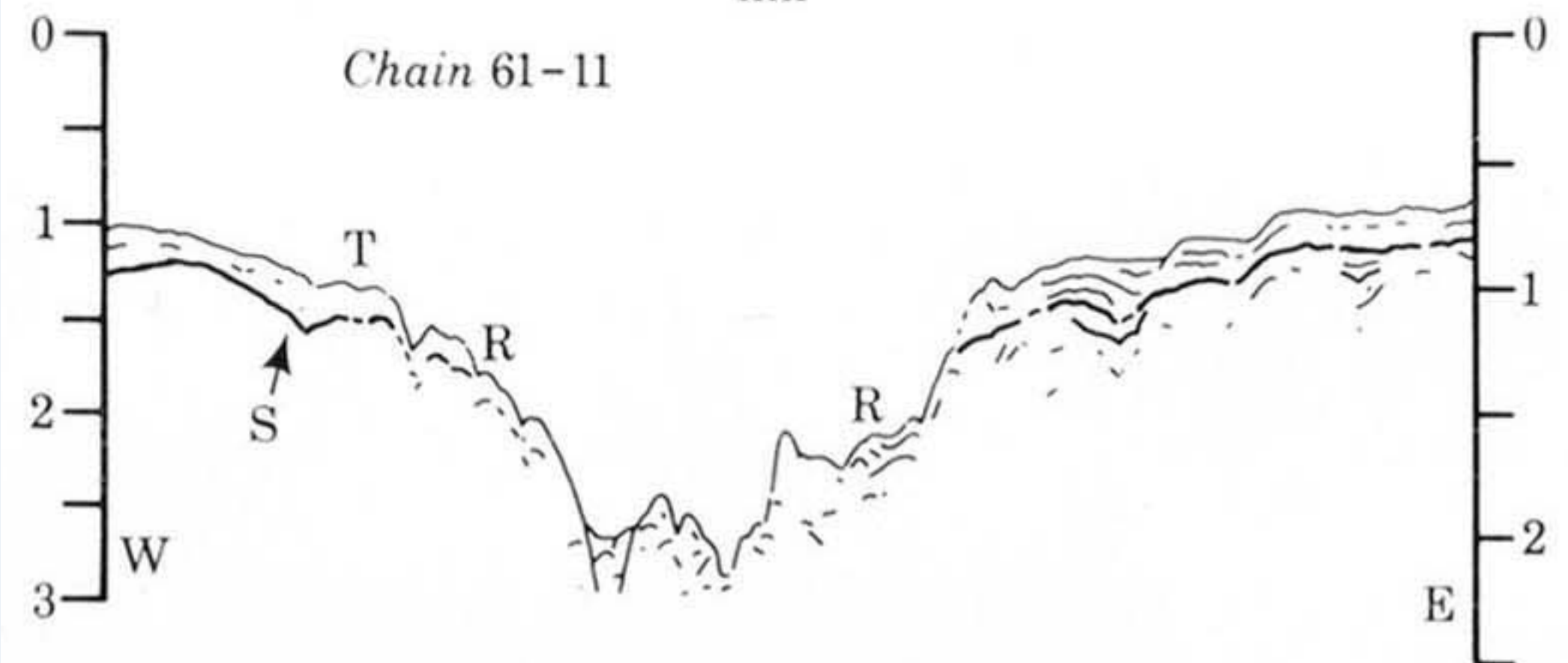
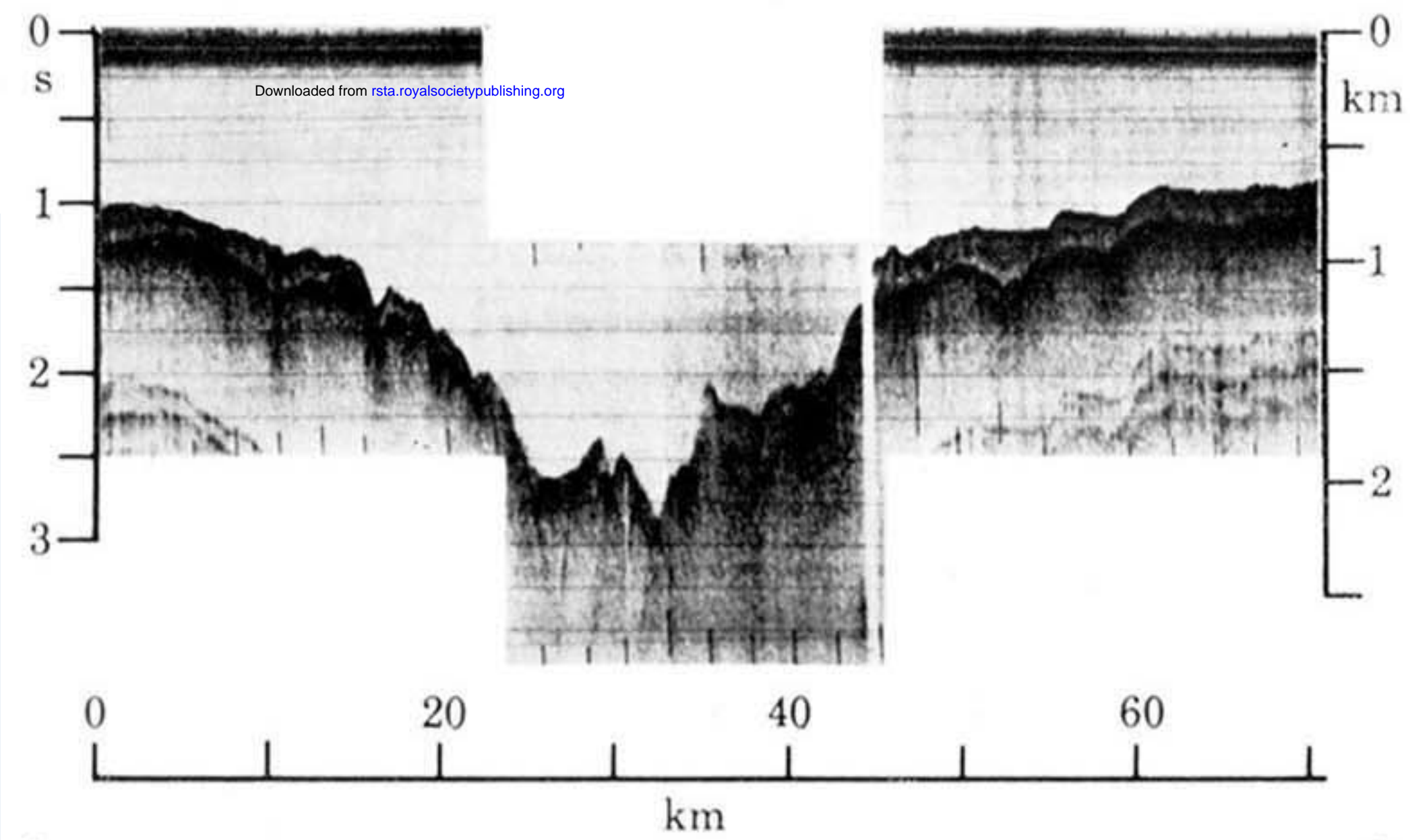
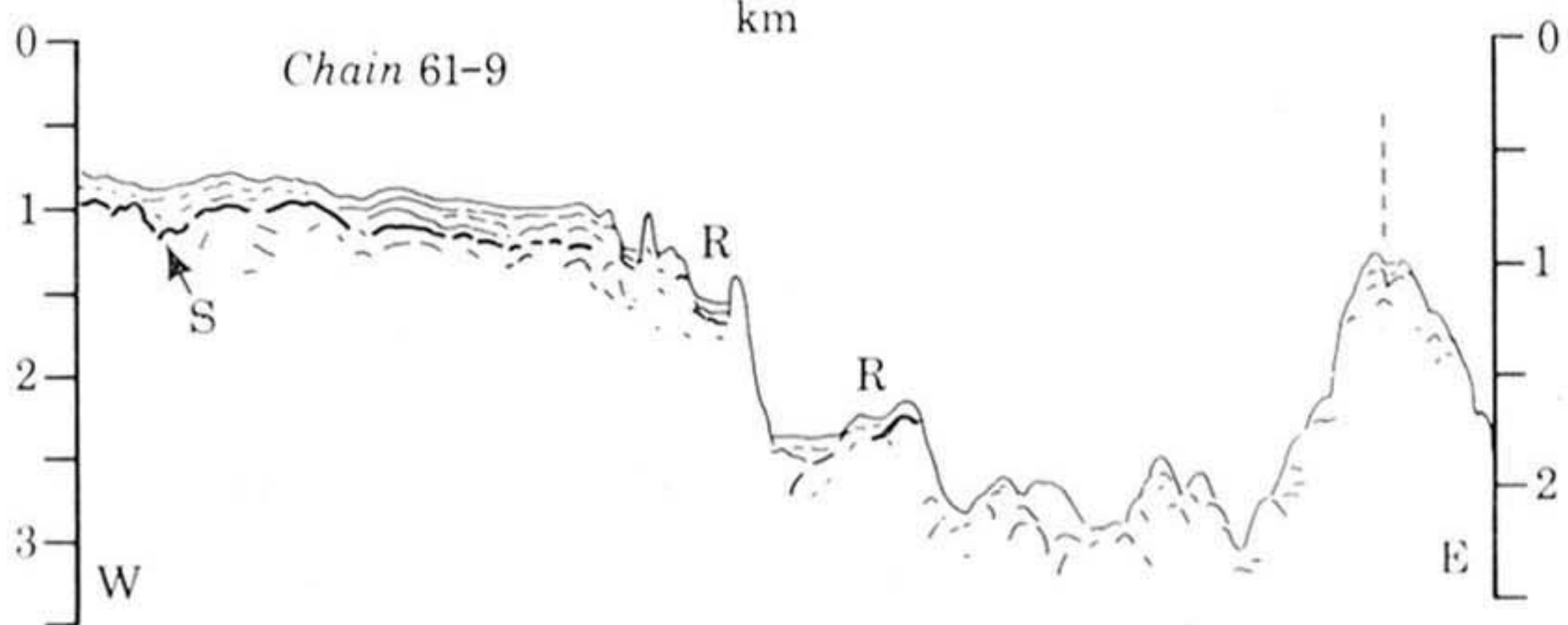
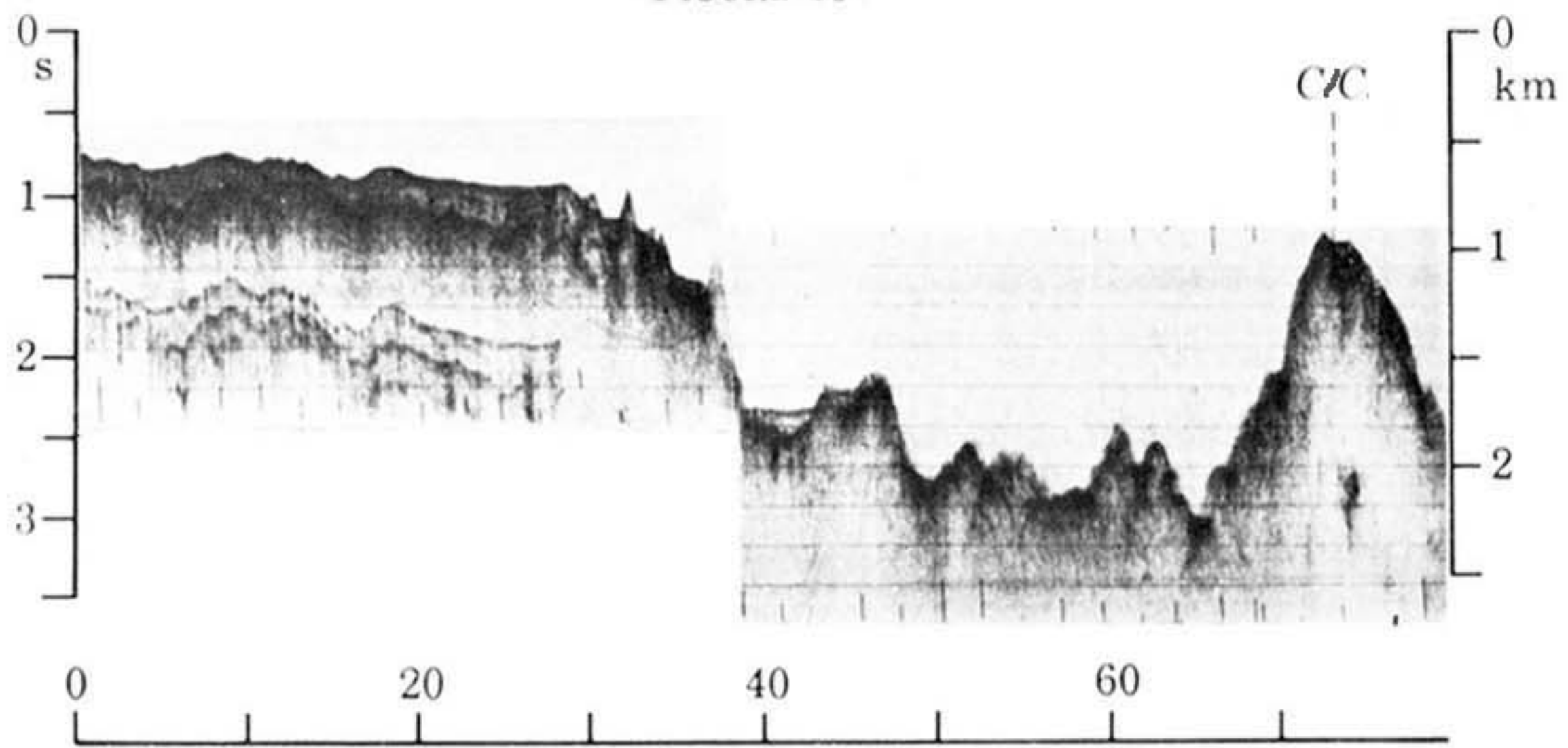


FIGURE 12

FIGURE 11

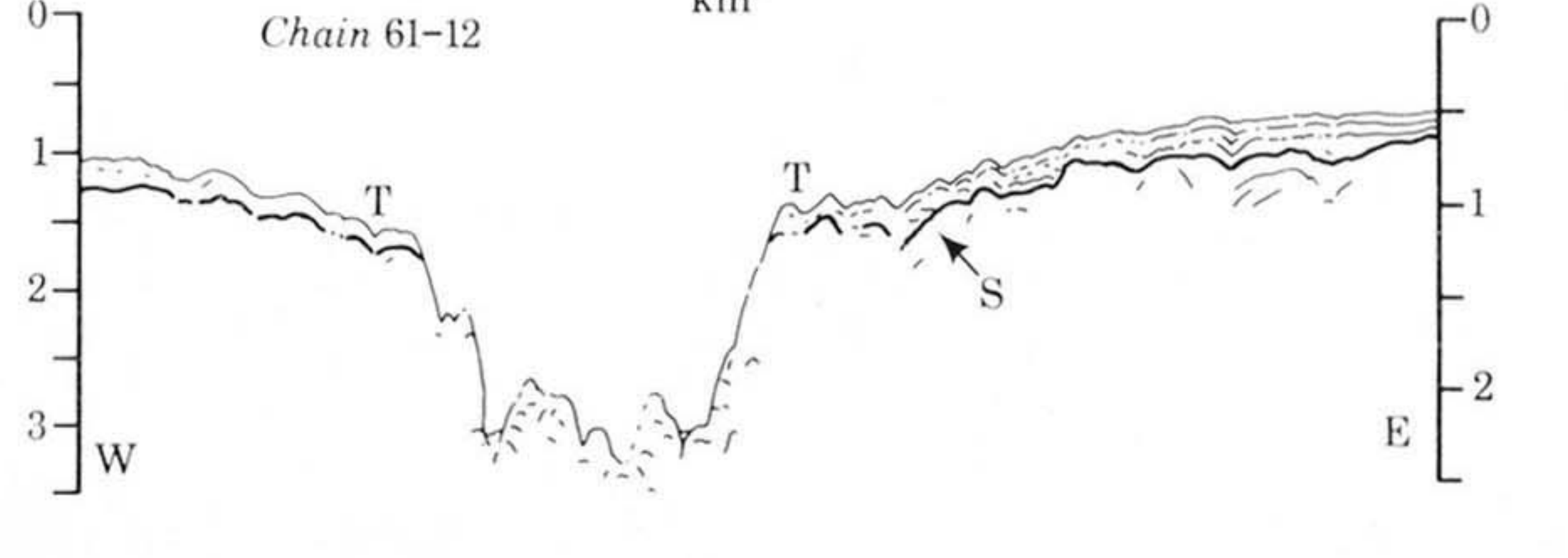
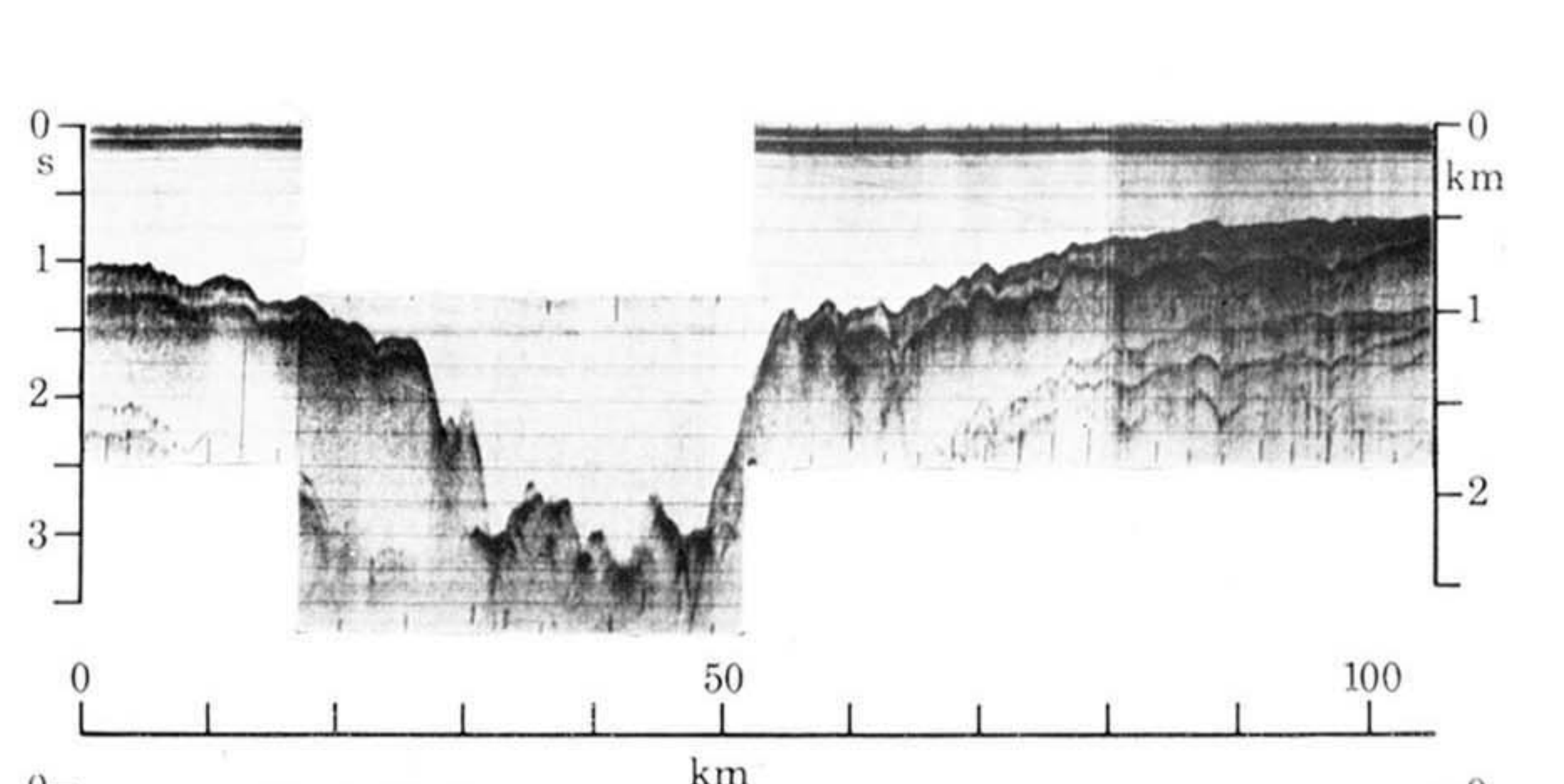
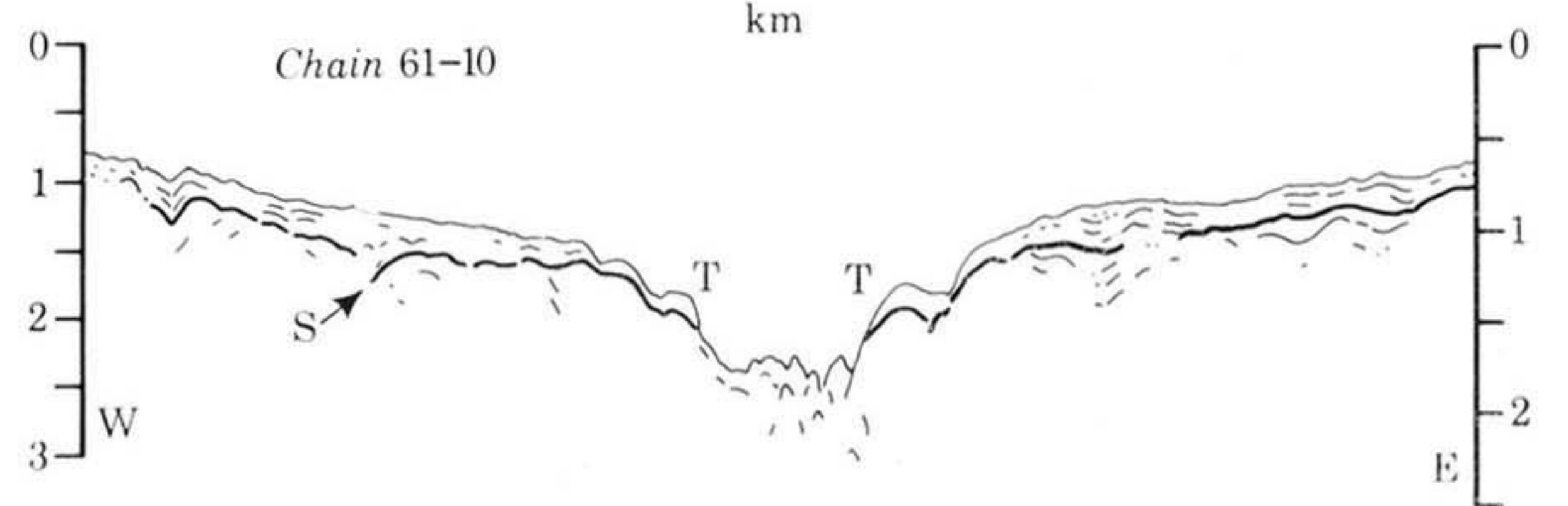
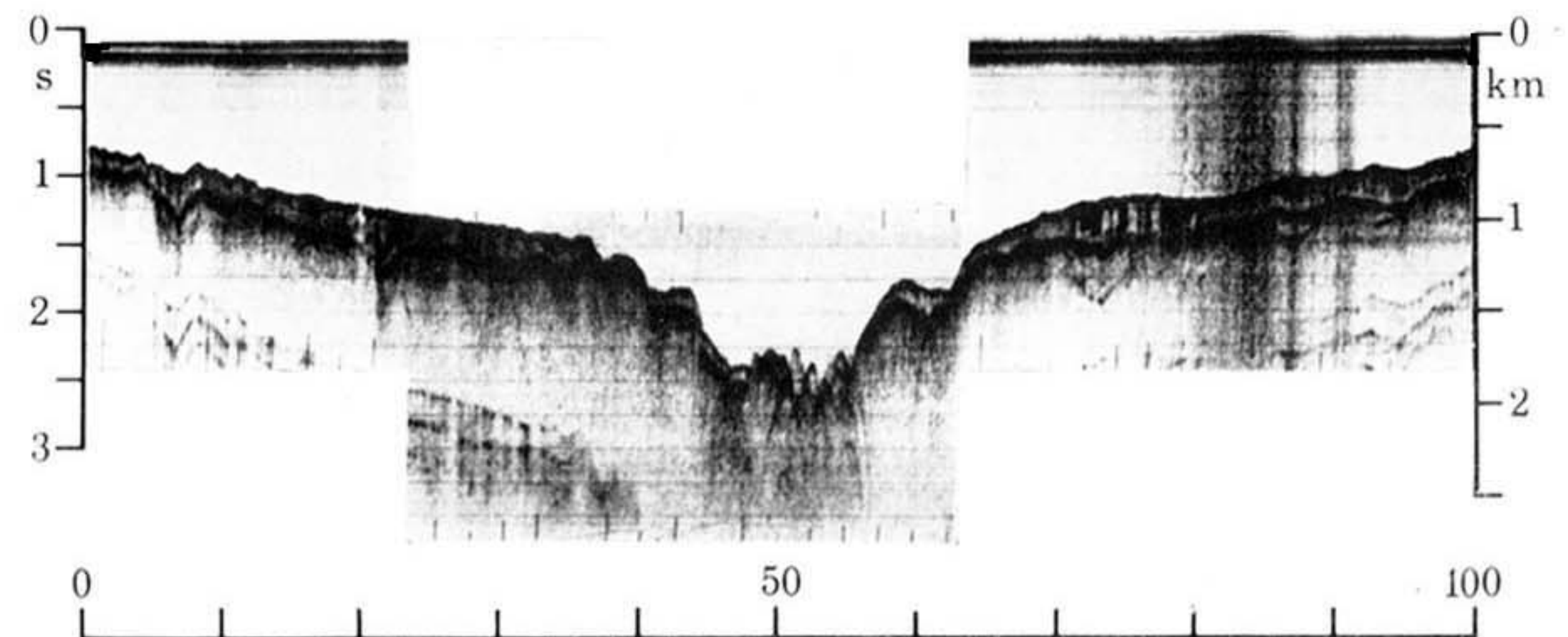
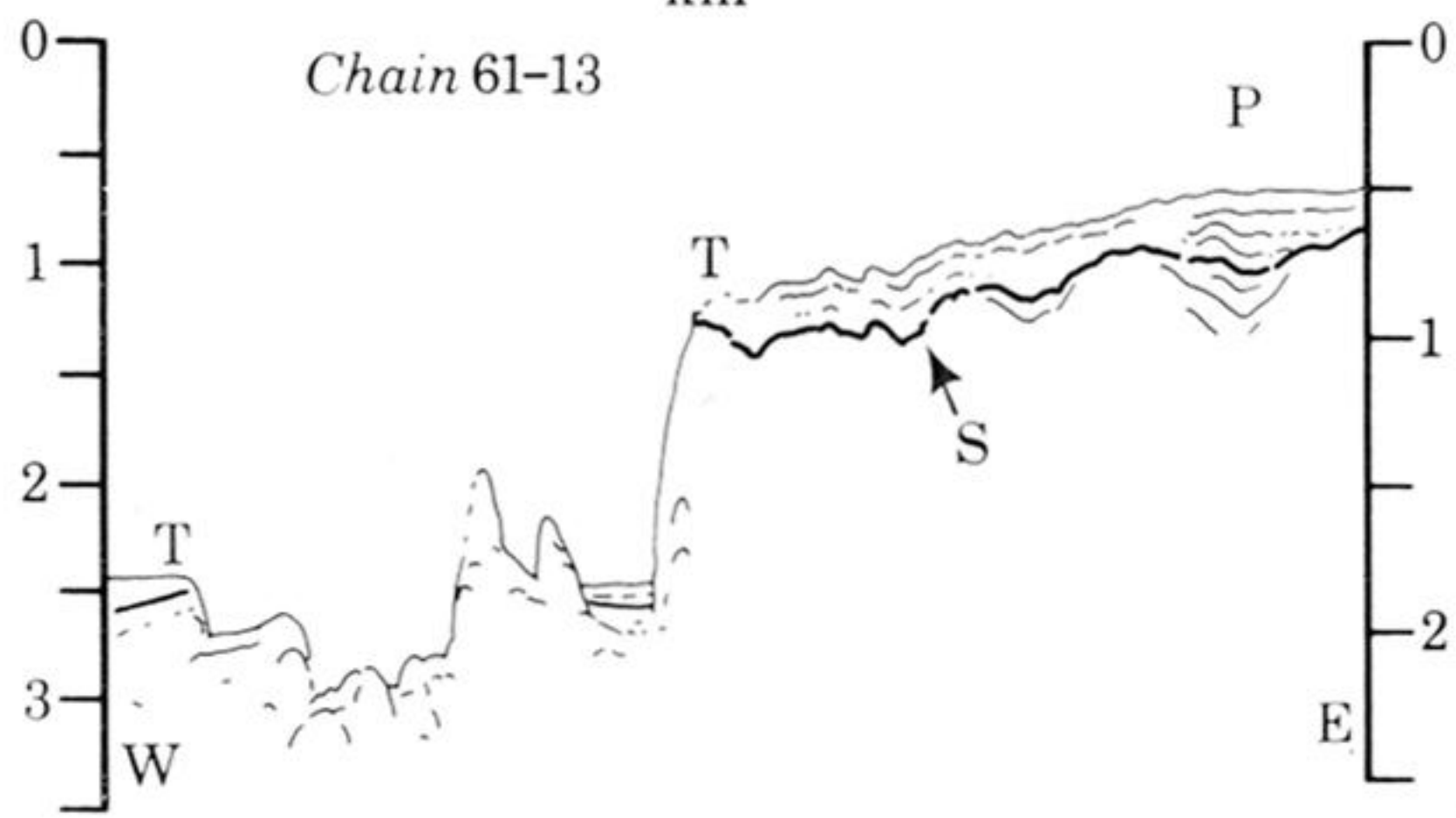
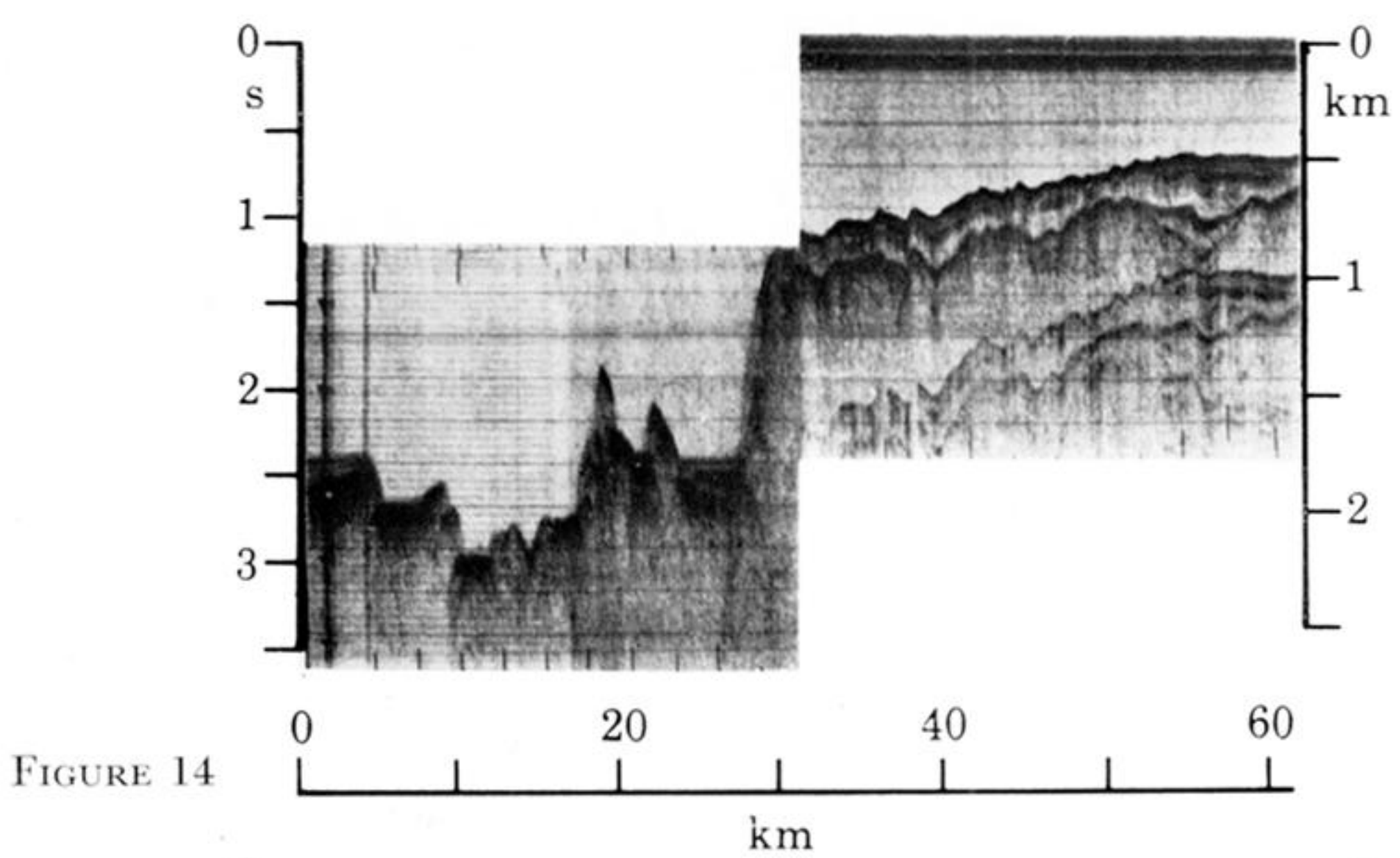
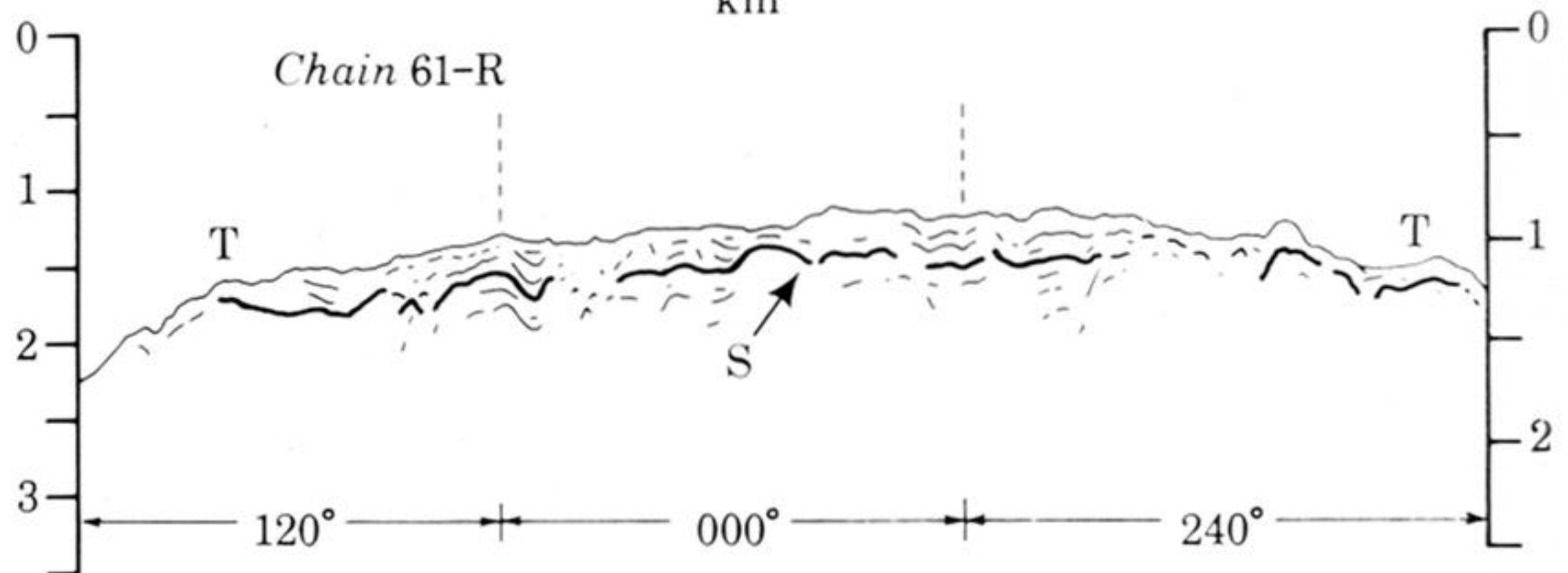
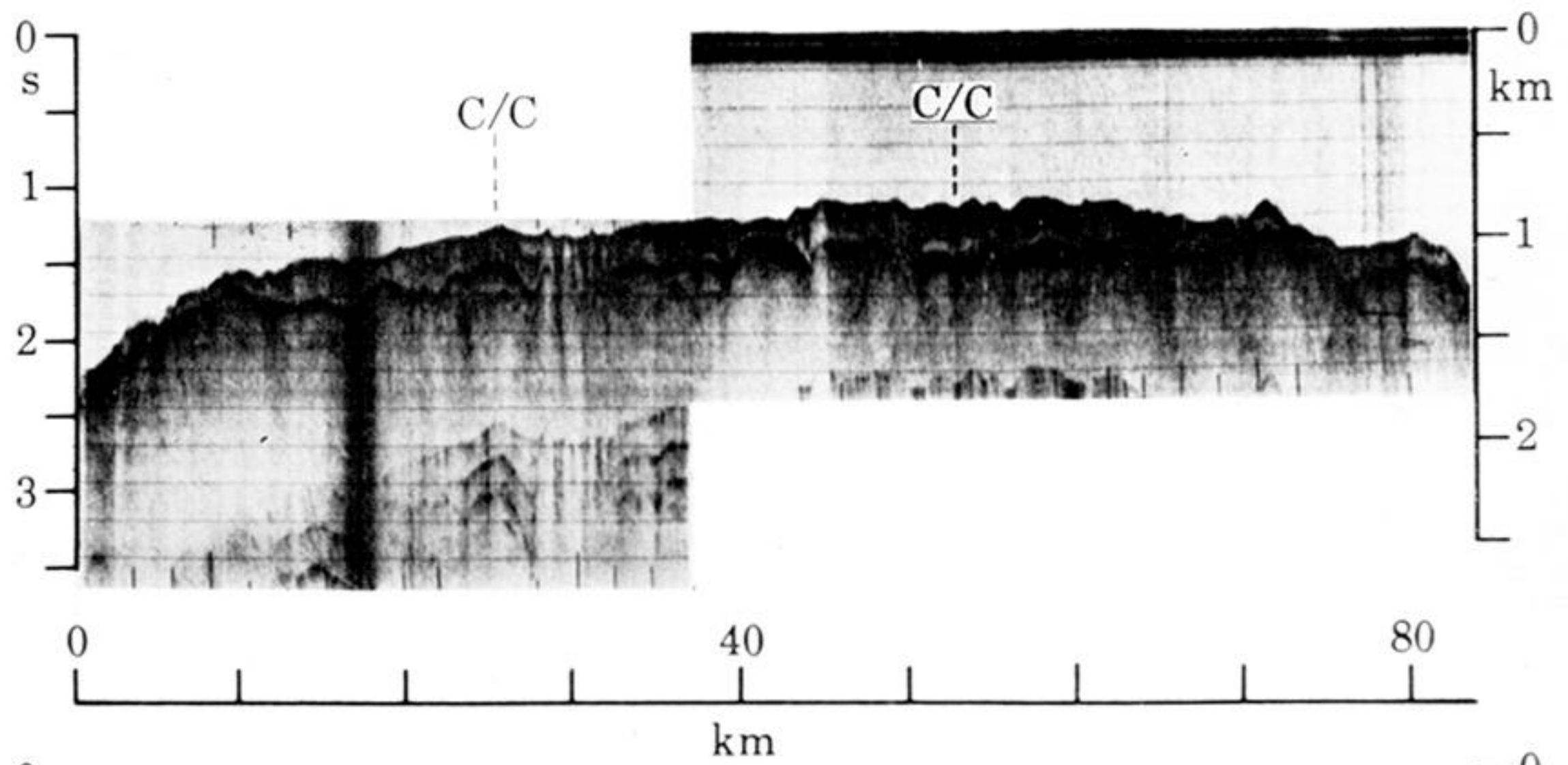


FIGURE 13

For legends see p. 146.



Downloaded from rsta.royalsocietypublishing.org



For legends see p. 146.

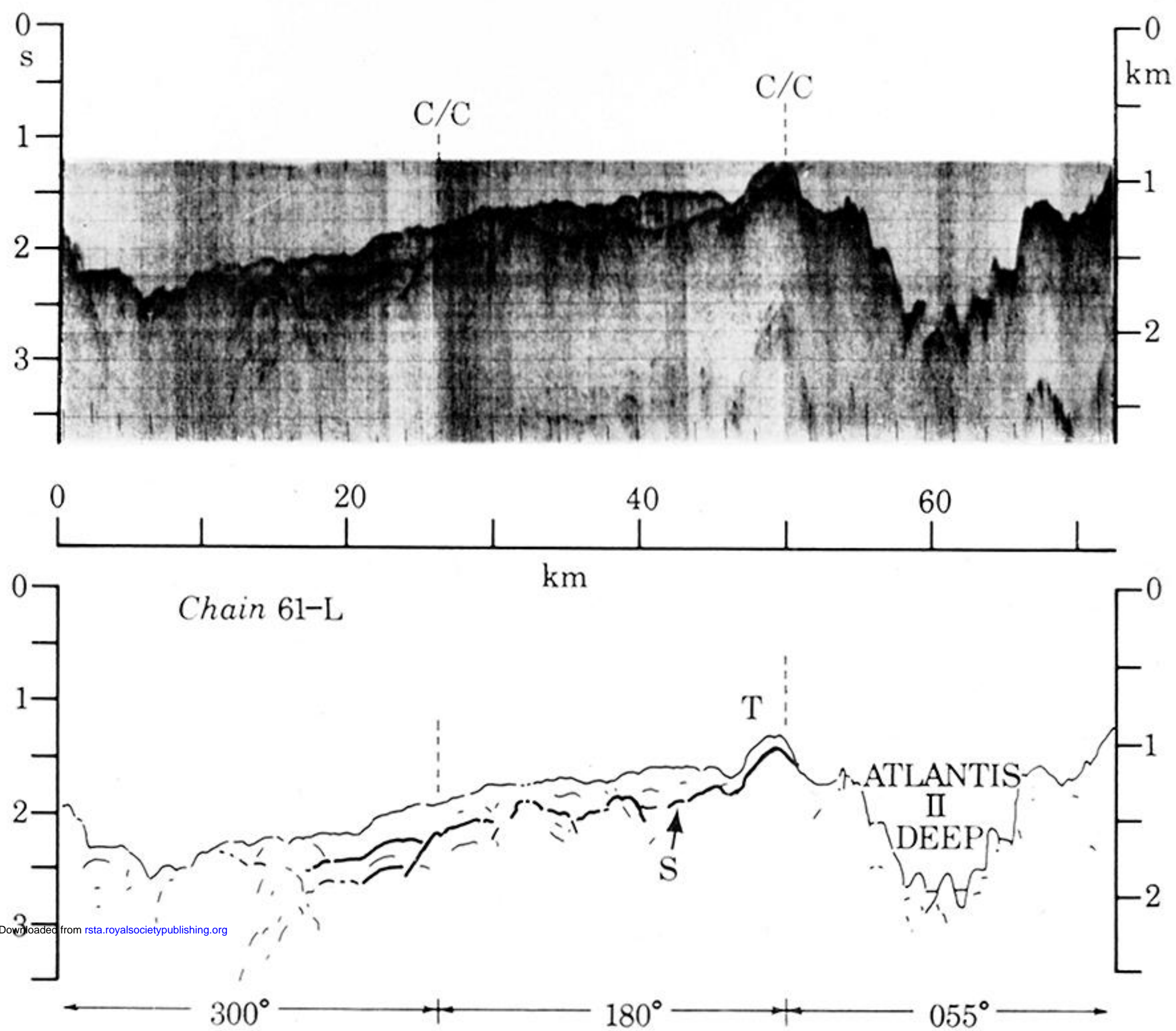


FIGURE 16 (after Ross *et al.* 1969). For legend see p. 146.

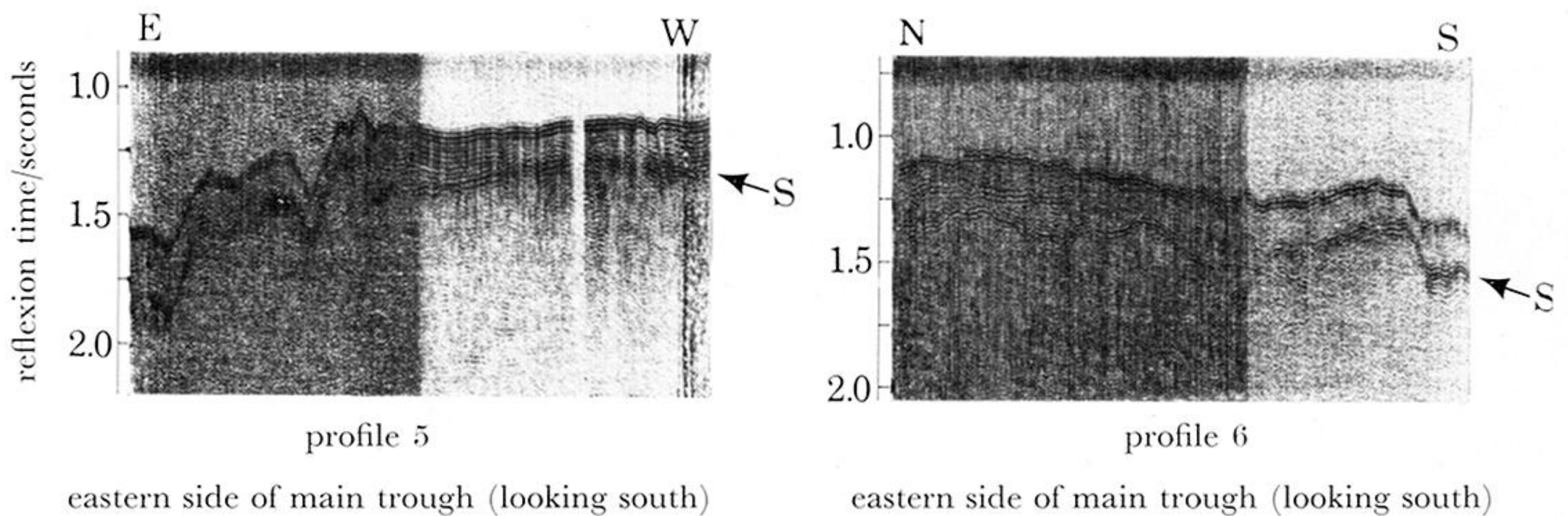


FIGURE 19. Photographs of selected *Chain 43* seismic reflexion records across the transitional region between the main trough and the axial trough near 24° N latitude (*a*) and 27° N latitude (*b*). The axial trough is toward the right and left margins of the figure. Note that the configuration of reflector S appears to shape the seafloor in the axial trough whereas in the main trough (centre of figure) the rugged nature of reflector S is not seen in the seafloor topography. Also the lack of internal reflectors in the material above reflector S near the axial trough demonstrates the relative transparency of this material as compared to that of the adjacent layered sequences in the main trough.

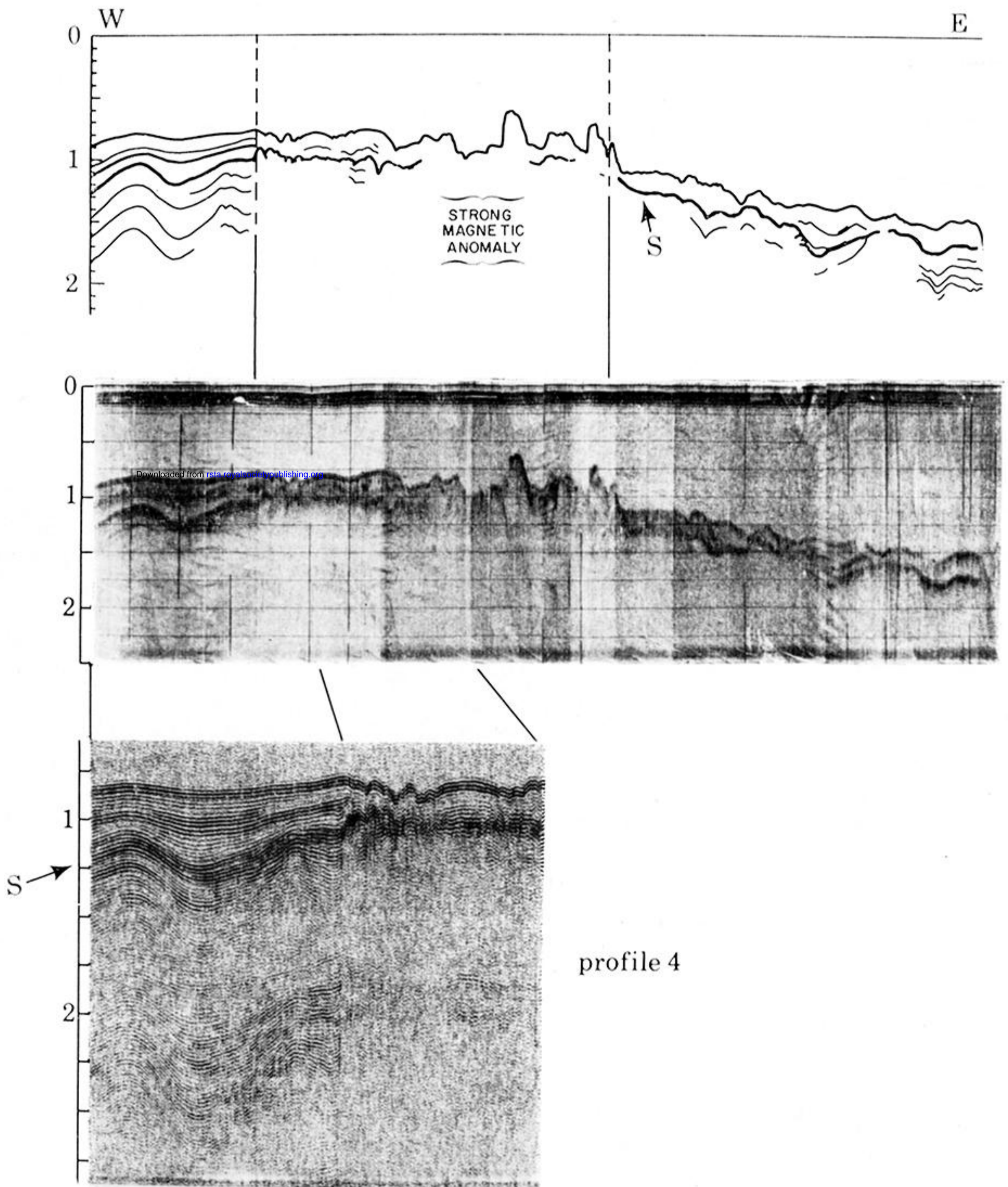
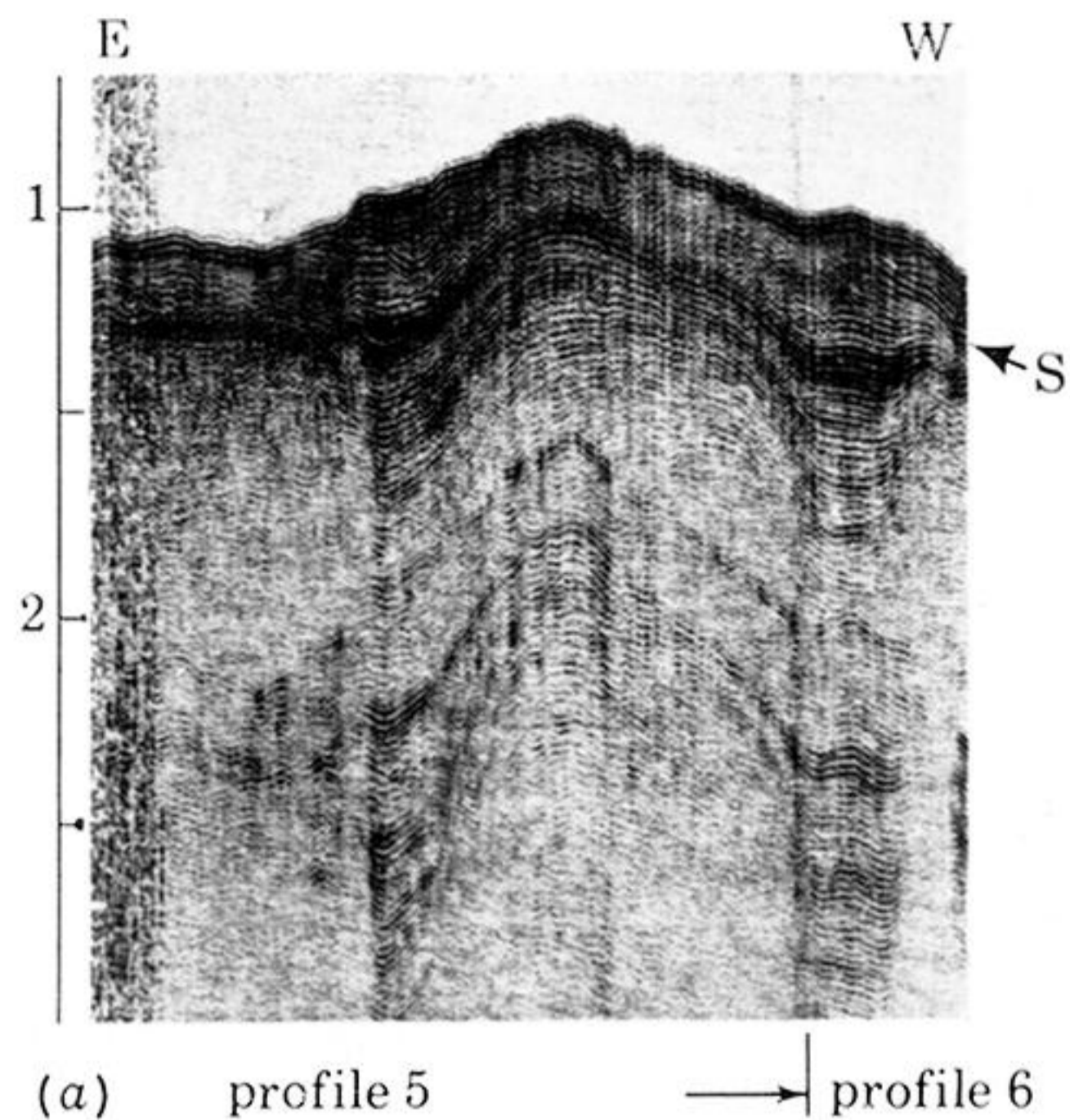


FIGURE 17. Western part of seismic profile 4 of *Chain Cruise 43*: (top) line drawing interpretation; (middle) seismic reflexion record, recording bandwidth 37.5 to 300 Hz; (bottom) section of reflexion record, recording bandwidth 37.5 to 75 Hz. (After Knott *et al.* 1966, figure 2.)



Downloaded from rsta.royalsocietypublishing.org

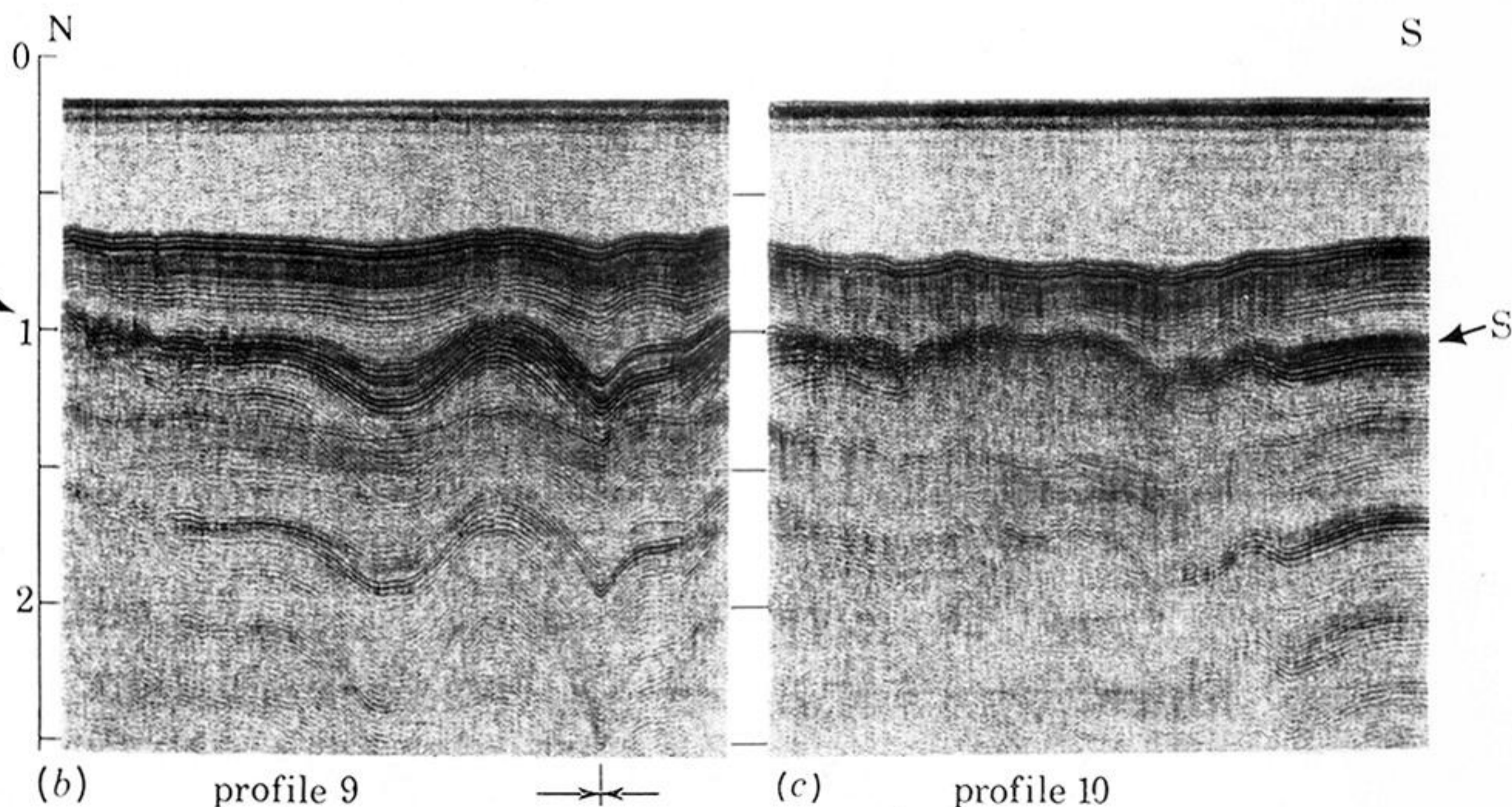


FIGURE 18. Photographs of selected *Chain Cruise 43* reflexion records. (a) Western margin of the main trough at 24° N latitude. The anticline appears to be bounded by a steeply dipping fault along its north side (left) which does not involve the layers above reflector S. (b) and (c) show the western margin of the main trough near 18° N latitude. Note that reflector S appears to be more strongly folded than the sediment layers directly beneath the seafloor to profile 9. In each of these profiles, reflector S, 0.25 to 0.50 s below the seafloor, is believed to be the Mio-Pliocene contact (after Knott *et al.* 1966).